Relative contribution of the pKpVP plasmid and the GIE492 and ICEKp10 genomic islands to the *Klebsiella pneumoniae* virulence over the zebrafish host model

Tesis

Entregada A La
Universidad De Chile
En Cumplimiento Parcial De Los Requisitos
Para Optar Al Grado De

Magíster en Ciencias Biológicas

Facultad De Ciencias

Por

Matías Ignacio Gálvez Silva

Enero, 2023

Director de Tesis Dr. Andrés Marcoleta Caldera
Codirectora de Tesis: Dra. Macarena Varas Poblete

FACULTAD DE CIENCIAS

UNIVERSIDAD DE CHILE

INFORME DE APROBACION

TESIS DE MAGÍSTER

Se informa a la Escuela de Postgrado de la Facultad de Ciencias que la Tesis de Magíster presentada por el candidato.

Matías Ignacio Gálvez Silva

Ha sido aprobada por la comisión de Evaluación de la tesis como requisito para optar al grado de Magíster en Ciencias Biológicas, en el examen de Defensa Privada de Tesis rendido el día …….

Director de Tesis:
Dr. .....

Co-Directora de Tesis
Dra. .....

Comisión de Evaluación de la Tesis

Dr. .....

Dr. .....

A mi familia y también a mis abuelos, que, aunque no están, esto es gracias a ellos.

BIOGRAFÍA

Desde pequeño he sentido interés y curiosidad en entender cómo suceden las cosas. Con el transcurso de los años, eso me llevó a dedicarme a las ciencias y tras algo de incertidumbre, comencé a estudiar licenciatura en biología en Juan Gomez Millas. A medida que avanzaba en los ramos llegué a conocer la microbiología, área que me cautivó y por la cual decidí continuar a mis estudios de postgrado. Todo mi paso por la facultad ha significado un crecimiento tanto académico como personal, en el cual he aprendido a sortear diversas dificultades. Hoy al terminar este proceso y observar lo que he avanzado, valoro el esfuerzo y el compromiso que dediqué a mi trabajo.

AGRADECIMIENTOS

Mi paso por el programa de Magíster y el desarrollo de esta Tesis no estuvo exenta de desafíos que tuve que aprender a sortear. Desde el primer momento nos vimos enfrentados a una pandemia que desajustó completamente los planes y como tal, hubo que aprender a adaptarse. Sin embargo, la gente que me apoyó en este proceso fue de gran importancia para poder concluirlo de manera satisfactoria.

Por una parte, agradecer a todos los laboratorios con los que comparti y trabajé. Al grupo del Dr. Miguel Allende, con mención especial al bioterio de peces, donde Yari y Fran me recibieron para el aprendizaje del manejo y uso del modelo zebrafish. Al Dr. Francisco Chávez, que además de aportar con ideas y discusiones nos facilitó las dependencias y equipamientos de su laboratorio, SysMicrolab, donde desarrollé buena parte de los experimentos de este trabajo. Y por su puesto, el laboratorio de Biología Estructural y Molecular, lugar donde fui recibido por mis tutores Macarena Varas y Andrés Marcoleta, los cuales me han ayudado de gran manera en el desarrollo de mis habilidades y pensamiento crítico para trabajar en ciencia. Además de agradecer a todos los compañeros del BEM por su gran apoyo y buen ambiente de trabajo, en especial a Camilo y Valentina que en periodos de pandemia éramos los únicos que rondábamos el laboratorio y fueron fuente de respuestas científicas y gratos momentos.

Agradecer también a mis amigos por todo su apoyo, comprensión, almuerzos, risas, café y cervezas que siempre fueron un oasis de distracción en muchos momentos de estrés y cansancio.

Finalmente, quiero agradecer a mis padres y hermanos, quienes siempre depositaron su confianza y cariño en mí; por aguantar tantas malas caras y desánimos cuando las cosas no iban tan bien, por ese apoyo incondicional, por estar siempre pendientes y disponibles con alguna palabra alentadora, por sus consejos y recomendaciones. También, agradecer a Belén que apareció en la parte final de este camino, pero que ha sido fundamental en los momentos más difíciles, de verdad muchas gracias. Esta tesis se realizó conjuntamente en el Laboratorio de Biología Estructural y Molecular y el Laboratorio de Microbiología de Sistemas, ambos de la facultad de ciencias de la Universidad de Chile, bajo la dirección del Dr. Andrés Marcoleta y la codirección de la Dra. Macarena Varas.

La tesis contó con financiamiento del proyecto FONDECYT 11181135

INDEX

LIST OF TABLES

LIST OF FIGURES

LIST OF SYMBOLS, ABBREVIATIONS OR NOMENCLATURE

°C: Degrees Celsius

Car: Carbenicillin

CFU: Colony forming unit

Cir: Catechol siderophore receptor

clb: gene coding for colibactin

DNA: Deoxyribonucleic acid

FepA: Catechol siderophore receptor

Fiu: Catechol siderophore receptor

g: Gram

GIE492: Genomic Island E492

GFP: Green fluorescence protein

h: Hour

HIF: Hypoxia inducible factor

Hpe: Hours post exposition

Hpf: Hours post fecundation

HvKp: Hipervirulent *Klebsiella pneumoniae*

iro: gene coding for salmochelin siderophore

iuc: gene coding for aerobactin siderophore

ICEs: Integrative conjugative elements

ICEKp10: Integrative conjugative element Kp10

ICEKp1: Integrative conjugative element Kp1

Kan: Kanamicin

kDa: Kilodalton

L: Liter

LMP: Low melting point

LPS: Lipopolysaccharide

LB: Luria-Bertani

Min: Minutes

MGEs: Movile genetic elements

mL: Microlitres

mM: Milimolar

MOI: Multiplicity of infection

OD600: Optical density at 600 nanometers

PBS: Phosphate buffered saline

pKpVP: *Klebsiella pneumoniae* virulence plasmid

rmpA: gene coding for RmpA protein

rmpC: gene coding for RmpC protein

rmpD: gene coding for RmpD protein

RFP: Red fluorescence protein

SASP: Senescence-associated secretory phenotype

µg: Microgram

µL: Microlitres

ybt: gene coding for yersiniabactin siderophore

RESUMEN

La transferencia horizontal de genes y los elementos genéticos móviles (EGMs) juegan un papel fundamental en el desarrollo de patógenos bacterianos que presentan rasgos fenotípicos de relevancia clínica, como por ejemplo, resistencia a antibióticos o una mayor dotación de factores de virulencia. Este es el caso de cepas hipervirulentas de *Klebsiella pneumoniae*, causantes de abscesos hepáticos y otras infecciones metastásicas graves, las cuales cuentan con diversos genes asociados a la virulencia, parte de los cuales están codificados en EGMs. En particular, dichas cepas frecuentemente portan las islas genómicas GIE492 e ICEKp10, y el plásmido de virulencia pKpVP, aunque se desconoce la contribución relativa de cada uno de estos EGMs en distintas etapas del proceso infectivo. Hasta la fecha, el estudio de estas cepas hipervirulentas se ha descrito en modelos de hospedero mamíferos, los cuales presentan una serie de limitaciones éticas y de infraestructura. Por ello, tomando en cuenta las ventajas que ofrece el modelo *Danio rerio* (pez cebra) y que sus larvas han sido usadas como hospedero de otras cepas de *K. pneumoniae* (no hipervirulentas), en esta Tesis se propuso estudiar la contribución relativa de estos EGMs en el proceso infeccioso de la cepa hipervirulenta modelo *K. pneumoniae* SGH10, usando larvas de pez cebra como modelo de hospedero. Para ello, se usaron métodos de infección por inmersión estática y microinyección localizada en la vesícula ótica, determinando que el modelo de pez cebra es adecuado para el estudio de estas cepas. Además, se observó que la capacidad de esta cepa de generar infecciones extraintestinales

reportada en mamíferos se recapitula en el modelo de pez cebra. Respecto a la contribución de los EGMs bajo estudio en la virulencia mediante ensayos de inmersión, no se observaron diferencias significativas en la colonización intestinal ni en la letalidad de la cepa SGH10, comparada con mutantes que carecen de uno o más EGMs. Junto con esto, en los ensayos de microinyección se determinó que la cepa que carece del plásmido pKpVP presentó un menor grado de virulencia. En relación a la respuesta del sistema inmune ante las infecciones con estas cepas se observó que la mutante ΔICEKp10-GIE492 y la cepa curada del plásmido pKPvP presentaron un menor reclutamiento de neutrófilos en el sitio de infección, lo que sugiere que uno o más factores codificados en dichos EGMs contribuyen a la inmunogenicidad de estas cepas.

ABSTRACT

Horizontal gene transfer and mobile genetic elements (MGEs) play a fundamental role in the development of bacterial pathogens that present clinically relevant phenotypic traits, such as antibiotic resistance or an increased number of virulence factors. This is the case of hypervirulent strains of *Klebsiella pneumoniae*, causing liver abscesses and other severe metastatic infections, which have several virulence-associated genes, part of them encoded in EGMs. In particular, such strains frequently carry the genomic islands GIE492 and ICEKp10, and the virulence plasmid pKpVP, although the relative contribution of each of these EGMs at different stages of the infectious process is unknown. To date, the study of these hypervirulent strains has been described in mammalian host models, which present several ethical and infrastructural limitations. Therefore, taking into account the advantages offered by the *Danio rerio* (zebrafish) model and that its larvae have been used as a host for other (non-hypervirulent) *K. pneumoniae* strains, in this Thesis, we proposed to study the relative contribution of these EGMs in the infectious process of the hypervirulent *K. pneumoniae* SGH10 model strain, using zebrafish larvae as a host model. For this purpose, methods of infection by static immersion and localized microinjection in the otic vesicle were used, determining that the zebrafish model is suitable for studying these strains. In addition, it was observed that the ability of this strain to generate extraintestinal infections reported in mammals is recapitulated in the zebrafish model.

Regarding the contribution of the EGMs under study in virulence by immersion assays, no significant differences were observed in intestinal colonization or lethality of strain SGH10 compared to mutants lacking one or more EGMs. Conversely, in microinjection assays, it was determined that the strain lacking the pKpVP plasmid presented a lower degree of virulence. In addition, regarding the immune system's response to infections with these strains, the ΔICEKp10-GIE492 mutant and pKpVP-cured strain presented lower recruitment of neutrophils at the site of infection, suggesting that one or more factors encoded in these EGMs would contribute to the immunogenicity of hypervirulent *K. pneumoniae*.

1 INTRODUCTION

1.1 *Klebsiella pneumoniae*

Klebsiella pneumoniae is a Gram-negative Enterobacteriaceae species found in various environmental conditions and associated with mammalian mucosal surfaces. From a clinical point of view and given its opportunistic nature, it is highly related to nosocomial infections mainly associated with the urinary tract, bacteremia, and pneumonia (Podschun & Ullmann, 1998; Prokesch et al., 2016). Several virulence and resistance factors appear to be common in these classical strains, including efflux pumps, fimbriae, lipopolysaccharides (LPS), capsule, and siderophores. About 80 to 90% of *Klebsiella pneumoniae* strains contain the $bla_{\text{SHV-1}}$ β-lactamase gene that confers resistance to ampicillin and carbenicillin antibiotics (Chaves et al., 2001). Furthermore, around the 1980s, strains resistant to multiple antimicrobial compounds began to appear, partly due to the ability of this species to acquire resistance genes through horizontal transfer and the strong pressure caused by the misuse of antibiotics in the hospital environment (Paczosa & Mecsas, 2016; Pendleton et al., 2013).

1.2 Hipervirulent *Klebsiella penumoniae* (hvKp)

In the 1980s, Asian patients with pyogenic liver abscesses produced by *Klebsiella pneumoniae* strains, which also could spread metastatically, began to appear. These strains, when isolated on Luria-Bertani agar plates, had a hypermucoviscous phenotype,

which implies a positive string test, which means the ability to generate a viscous string >5mm when touched with a microbiology loop (Shon et al., 2013). Although the first appearances of these strains were associated with Asia, reports of cases have increased in different regions of the planet including North America, Europe, South America, Oceania (Decré et al., 2011; Fierer et al., 2011; Turton et al., 2007; Vila, 2011). Clinically, these strains can generate community-acquired infections in patients with no apparent comorbidity. These infections have the singularity to generate metastasic infections from intestinal colonization, characteristically producing pyogenic liver abscesses, meningitis, and endophthalmitis, among others (Choby et al., 2020; Ye et al., 2016).

Phylogenetic analyses based on approximately 2000 core genes have shown that there are hundreds of clonal groups of *Klebsiella pneumoniae*, which can be distinguished based on their accessory genome content. This accessory genome has been developed due to horizontal gene transfer directed by chromosomal recombination and plasmid-mediated conjugation, as well as integrative conjugative elements (ICEs). These events have generated a great diversity of *K. pneumoniae* lineages. Within these, a number of clones produced represent a health hazard to both animals and humans. There are clonal groups encompassing strains resistant to multiple antimicrobial compounds, which are generally associated with hospital environments, and hypervirulent lineages, causing community-acquired metastatic infections (Wyres et al., 2020). The phylogeny of 97 geographically diverse hvKp isolates showed that a high proportion (83.5% of all isolates studied) belonged to the CG23-I sublineage, which harbored several virulence factors associated with mobile gene elements (MGEs) (Lam, et al., 2018). MGEs are DNA segments, some

carrying virulence or resistance-associated genes, which may or may not integrate into the bacterial chromosome and could be transferred horizontally (Malachowa & Deleo, 2010). In particular, two genomic islands and one virulence plasmid were associated with the CG23-I sublineage. First, the ICEKp10 island, containing the *ybt* (siderophore yersiniabactin) and *clb* (colibactin genotoxin) genes, and second, the GIE492 island comprising the gene cluster to produce the antibacterial peptide microcin E492 (MccE492) and the salmochelin siderophores. On the other hand, the virulence plasmid pKpVP contains the *rmpA*, *rmpC* and *rmpD* genes involved in the hypermucoviscous phenotype, along with the *iro* and *iuc* genes associated with the production of salmochelin and aerobactin siderophores, respectively (Lam, Wyres, Judd, et al., 2018). Although some of these genes encode known *K. pneumoniae* virulence factors, the relative contribution of ICEKp10, GIE492, and pKpVP to the hvKp virulence remains unknown, obscuring which of them suppose a higher risk upon acquisition by a *K. pneumoniae* strain.

1.2.1 Virulence Factors associated with hypervirulent *Klebsiella pneumoniae*

Pathogenicity on the host is determined by the ability of the microorganism to cause damage. Thus, virulence can be understood as relative capacity of generating damage, because of the dependence of a susceptible host. Taking into account these considerations, virulence factors are microbial components that alter the microorganism-host interaction, increasing the level of damage due to the capacity they confer to face the response of the affected organism (Casadevall & Pirofski, 2009). This includes not only those components that directly cause damage to cells or tissues but also those molecules that allow evasion

or modulation of host defense systems (Johnson, 2017). Thus, different categories of virulence factors can be observed according to the potential they confer, such as the ability to enter the host, evade its defenses, counteract the immune system response, and the possibility to acquire iron and nutrients from the environment, among others (Casadevall & Pirofski, 2009).

Considering the above, *Klebsiella pneumoniae* strains have different and diverse virulence factors, including different siderophore systems. Siderophores are low molecular weight molecules (400-1000 kDa) with a high affinity for iron produced by these organisms under iron-deficient environmental conditions (Saha et al., 2012). The importance of these factors relies on the fact that iron is an essential element for the life of plants, animals, and microorganisms because it has ideal redox characteristics to participate in the electron transport chain and metabolic processes. However, there is low availability of Fe (III) in the environment. Therefore one of the strategies of plants, fungi and microorganisms for iron accumulation is the production of siderophores (Hider & Kong, 2010). As mentioned in the previous section, *K. pneumoniae* strains from different clonal groups associated with hypervirulence present different siderophore systems, such as salmochelin, yersiniabactin and enterobactin. These are associated with MGEs, so it is possible to find more than one of these systems in the different microorganisms (Lam et al., 2018; Wyres et al., 2020).

The capsule is another relevant factor mediating *K. pneumoniae* virulence. To date, 79 capsule serotypes have been described that can be found in the various strains of *Klebsiella*

pneumoniae (Pan et al., 2015). However, the hypervirulent strains are characterized by having mainly K1 or K2 serotypes (Yeh et al., 2010). Along with this, and as previously mentioned, another distinctive aspect is its hypermucoviscous phenotype. Capsule production and hypermucoviscosity have been related with evasion of the immune system response. Some evidence indicate that hypermucoviscocity acts mainly as an anti-adhesion factor, while capsule production mediates resistance to phagocytosis by macrophages and other immune cells. In any case, it should be noted that although they are different characteristics, capsule production is necessary to generate the hypermucoviscous phenotype (Walker et al., 2020).

The bacteriocin microcin E492 is an antimicrobial peptide with toxic activity against several Enterobacteriaceae species, which can be presented in two forms. An active form, post-translationally modified by the covalent binding to its C-terminus of a salmochelin molecule, or an unmodified (inactive) form. The bactericidal capacity of MccE492 lies in the formation of pores in the plasma membrane, acting mainly on bacterial cells expressing the catechol siderophore receptors FepA, Fiu and Cir that mediate their internalization into the periplasm of the target cell (Lagos et al., 2009; Lagos et al., 1993; Riley & Gordon, 1999). However, the role of the production of this peptide in the context of infection is unknown.

Additionally, colibactin is a genotoxic polyketide that induces DNA double-strand breaks. Its activity depends on direct contact with host cells and can cause cell cycle arrest or even apoptosis (Faïs et al., 2018; Taieb et al., 2016). So far, it is unclear whether colibactin

plays a role in the pathogenesis of hypervirulent strains of *K. pneumoniae*.

Among strains of this species studied as models of hvKp, *K. pneumoniae* NTUH K2044 was used for experimental work and infection assays. However, this strain does not encode colibactin determinants and has ICEKp1 instead of ICEKp10, which is more prevalent within CG23. More recently, the clinical isolate SGH10 was proposed as more representative of hvKp, which was obtained in 2014 from a liver abscess of a 35-year-old patient with no comorbidities from Singapore. This strain has the phylogenetic characteristics mentioned above, as well as the described mobile gene elements and virulence factors (Lam, et al., 2018).

1.3 Infection models to study *K. pneumoniae* pathogenesis

Historically, mammalian models have been used to study different aspects of pathogens' virulence. However, given their economic, instrumental, and ethical limitations, alternative host infection models have been developed. In this context, *Danio rerio* (zebrafish) has become a validated model for the study of host-pathogen interactions as well as human infectious diseases (Torraca et al., 2014; Varas et al., 2017; Vergunst & O'Callaghan, 2014). Among their advantages is the optical transparency that allows visualization of the infectious process *in vivo* in a non-invasive way. Also, the wide availability of transgenic lines having different fluorescence-labeled cell lineages enable observe physiological changes response to infections (Astin et al., 2017; Saraceni et al., 2016; Wang et al., 2019). In addition, this model has an innate immune system sharing conserved features with the immune system of mammals, including the major components

of the signaling pathways, and where about 70% of human genes have an orthologue in zebrafish (Howe et al., 2013; Stein et al., 2007).

The first immune response avialable during zebrafish development is the innate response, while the adaptive one is functional from the fourth-week post fertilization, allowing these responses to be studied separately (Benard et al., 2012; Meeker & Trede, 2008). This characteristic of the zebrafish larvae model allows to study how the components of the innate immune system (mainly macrophages and neutrophils) interact with various pathogens, including human pathogens. Macrophages capable of phagocytosing microorganisms have previously been recorded in zebrafish as early as 28 hours post fertilization (hpf), and functional neutrophils in larvae from 32 to 48 hpf have been recorded too (Harvie & Huttenlocher, 2015; Herbomel, 1999).

Previous work by our research group successfully used zebrafish larvae to compare the virulence of three strains of *K. pneumoniae*, measuring lethality, intestinal colonization and immune cell recruitment by static immersion experiments and bacterial injection into the otic vesicle (Marcoleta et al., 2018). However, although one of the strains showed increased virulence over zebrafish larvae, none corresponded to hypervirulent strains. Thus, further studies are required to test the utility of this host model in studying the pathogenesis of hvKp. Moreover, if suitable, this model could be used to study the contribution of the different characteristic mobile genetic elements associated with hvKp to the virulence of this priority bacterial pathogen.

Given the background described above, and considering that 1) hypervirulent *K. pneumoniae* are a critical concern pathogen 2) most hvKp carry the GIE492 and ICEKp10 genomic islands and the pKpVP plasmid 3) zebrafish larvae have shown to be a suitable model to study *K. pneumoniae* virulence and 4) we have access to the hypervirulent model strain *K. pneumoniae* SGH10 and mutant derivatives lacking the mentioned mobile elements; in this work, we propose to study the relative contribution of these mobile elements in the *K. pneumoniae* virulence over zebrafish larvae.

1.4 Hypothesis

Based on the described above, the following working hypothesis is proposed:

The mobile gene elements pKpVP, GIE492, and ICEKp10 contribute to hypervirulent *Klebsiella pneumoniae* pathogenesis over the zebrafish host model.

1.5 Objectives

1.5.1 General Objective

To evaluate the relative contribution of the mobile genetic elements pKpVP, GIE492, and ICEKp10 to the virulence of hypervirulent *K. pneumoniae* on zebrafish larvae.

1.5.2 Specific Objectives

1) To evaluate the role of the mobile genetic elements pKpVP, GIE492, and ICEKp10 on the hvKp lethality over zebrafish larvae.

2) To evaluate the role of the mobile genetic elements pKpVP, GIE492 and ICEKp10 on the hvKp intestinal and extra-intestinal colonization of zebrafish larvae.

3) To determine the contribution of the hvKp mobile elements pKpVP, GIE492, and ICEKp10 to elicit a zebrafish innate immune cell response.

2. MATERIALS AND METHODS

2.1 Bacterial strains and growth conditions

The Kp SGH10 strain was kindly provided by Prof. Yunn Hwen Gan from National University of Singapore. The mutant strains SGH10 ΔICEKp10, SGH10 ΔGIE492, SGH10 ΔICEKp10-GIE492, and the SGH10 pKpVP-cured strain were obtained previously by Dr. Andrés Marcoleta by mutagenesis procedure which was performed by assembly, conjugation, and homologous recombination of conditional suicide plasmids, for subsequent counter-selection with sucrose and tetracycline. This was performed following the protocol described by Tan et al. 2020

Table 1. Bacterial strains and plasmids used in this work

Bacterial strain or plasmid	**Genotype or comments**	**Source/Reference**
Klebsiella pneumoniae SGH10	Model hypervirulent strain isolated from a patient with liver abscess in Singapore (2014).	(Lam et al., 2018), available from ATCC. Kindly provided by Prof. Yunn Hwen Gan from the National University of Singapore.
Klebsiella pneumoniae SGH10 ΔGIE492	Deletion of the complete GIE492 genomic island	Laboratory collection
Klebsiella pneumoniae SGH10 ΔICEKp10	Deletion of the complete ICEKp10 genomic island	Laboratory collection
Klebsiella pneumoniae SGH10 ΔICEKp10-GIE492	Deletion of both genomic islands (GIE492 and ICEKp10)	Laboratory collection

Klebsiella pneumoniae SGH10 pKpVP-cured	Lacking the virulence plasmid pKpVP	Laboratory collection
Klebsiella pneumoniae SGH10 ΔwcaJ	Deletion of the *wcaJ* gene encoding a glycosyltransferase indispensable for capsule production.	Laboratory collection
Klebsiella pneumoniae DBS0305928 (KpGe)	Avirulent strain, previously used by our research group	Laboratory collection. Available from the Dicty Stock Center
pBBR-sfGFP	Constitutive expression of the sfGFP protein, Kan^r.	Kindly provided by Prof. Yunn Hwen Gan from the National University of Singapore.
pBBR-mApple	Constitutive expression of the mApple protein, Kan^r	Kindly provided by Prof. Yunn Hwen Gan from the National University of Singapore.

2.2 Growth conditions

Bacterial isolates were routinely grown in Luria-Bertani (LB) (10 g/L tryptone, 5 g/L yeast extract, 5 g/L NaCl) agar plates with the respective antibiotics at 37°C (Car 50 µg/mL, Kan 50 µg/mL). All work with bacteria was performed in a biosafety cabinet class II type a2, complying with all the necessary biosafety measures.

2.3 *Danio rerio* (zebrafish)

The embryos used were obtained from the fish hatchery ZAR-II managed by Dr. Miguel Allende's research group, complying with all the norms approved by the Ethics Committee of the Universidad de Chile. All the zebrafish embryos, Tab5 and transgenic line Tg(MPO:GFP) (Renshaw et al., 2006), were collected by natural spawning. Embryo

developmental stages are expressed in hpf.

The fertilized embryos were maintained at 28°C in E3 medium (5 mM NaCl, 0.17 mM KCl, 0.33 mM $CaCl_2$, 0.33 mM $MgSO_4$, equilibrated to pH 7.0, with methylene blue until 24 hpf in Petri dishes (50 embryos/dish) (Westerfield, 2000), maintaining a photoperiod of 14 h of light and 10 h of darkness. The embryo medium was replaced daily with clean medium.

2.4 Lethality assays

For lethality assays, an adaptation of the immersion infection protocol developed by Varas et al., 2017 was performed (Figure 1). This was carried out using 48 hpf Tab5 zebrafish larvae dechorionated using forceps and reserved until processing. In parallel, bacterial suspensions of strains *K. pneumoniae* SGH10, the mutant derivatives (ΔICEKp10, ΔGIE492, ΔICEKp10 ΔGIE492 (ΔICEKp10-GIE492), Δ*wcaJ),* KpGe and pKpVP-cured were made . When required for visualization by fluorescence microscopy, the strains were transformed with the pBBRsfGFP plasmid and then grown on LB plates with Car and Kan (50 µg/mL). First, bacterial suspensions were made in 50 mL falcon tubes with sterile E3 medium using sterile swabs to pick up and disperse the bacterial colonies and then shaking with vortex at maximum speed until complete homogenization. Then, the suspensions were adjusted to an optical density at 600 nm (OD600)=1.4 (equivalent to ~$1x10^9$ CFU/mL, according to viable bacteria recount by serial dilution and plating on LB-agar with the respective antibiotics). Afterwards, using 6-well plates, 10 to 15 larvae were deposited in wells containing 4 mL of sterile E3 medium and 4 mL of the bacterial

suspensions. Each condition was assayed in duplicates completing approximately 30 individuals, including the control condition only with sterile E3 medium (lacking bacteria).

The plates with infected larvae were incubated at 28°C for up to 48 h, keeping the respective photoperiod. Survival was recorded every three hours during the first 9 hours post exposition (hpe), and then recorded again at 24 hpe and 48 hpe. To evaluate the survival, tactile stimulation was performed on the tail of the individuals and visualization by Zeiss Stemi 305 stereomicroscope of the heartbeat when confirmation was needed. The dead larvae in each register were removed under the necessary biosecurity provisions.

Kaplan-Meier survival curves were constructed with the data obtained using GraphPad Prism version 8.0.1 software. Statistical analysis was performed with the same software using 2-way ANOVA tests with Bonferroni's multiple comparison post-test.

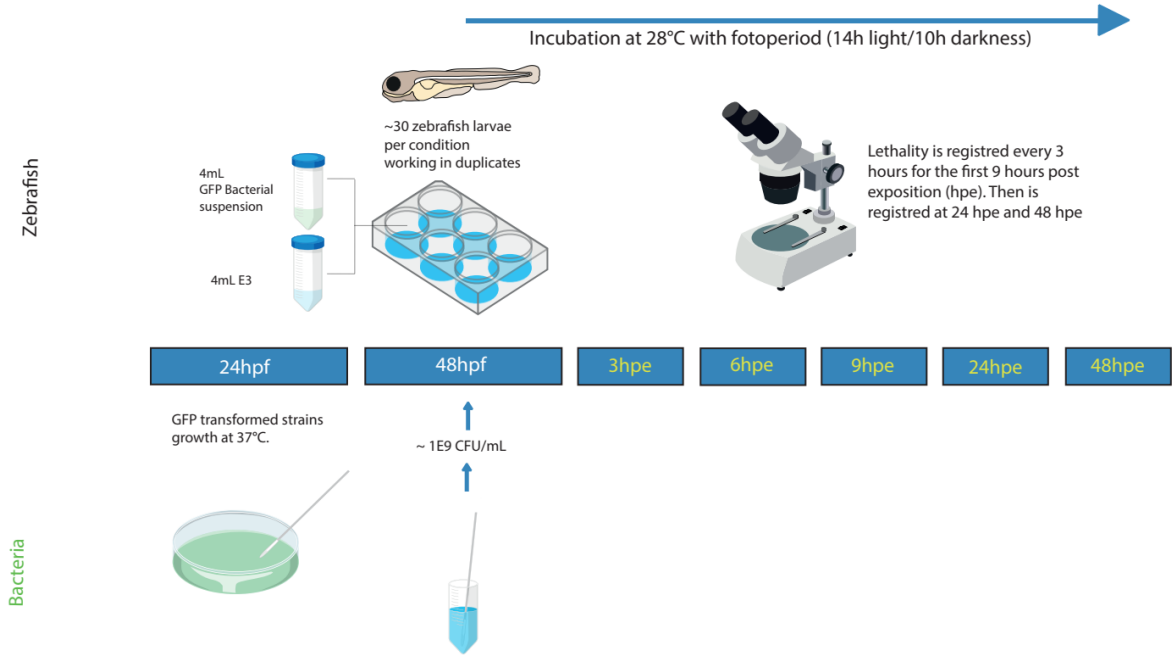

Figure 1. Workflow of the zebrafish larvae lethality assays to test the killing capacity of *Kp*SGH10,the mobile genetic elements mutants (ΔICEKp10, ΔGIE492, ΔICEKp10-GIE492) and pKpVP-cured strain over 48 hpf zebrafish larvae.

2.5 Intestinal colonization assays

These experiments were adapted from similar methods developed by Marcoleta et al., 2018 (Figure 2). Cell suspensions were obtained as described above, and the strains used were SGH10 WT, ΔICEKp10, ΔGIE492, ΔICEKp10-GIE492, pKpVP-cured and KpGe ,all strains used were transformed with the pBBR-sfGFP plasmid. The ΔwcaJ strain was not used in these assays because the report describing and validating this strain as an SGH10 avirulent mutantwas after the completion of this objective. Unfortunately, due to severe problems in the zebrafish hatchery caused by the COVID-19 pandemic, we were unable to obtain more larvae to test the mentioned mutant *a posteriori*

Ten to fifteen 72-hpf Tab5 zebrafish larvae were placed per well in a sterile 6-well plate with 4 mL of sterile E3 medium and 4 mL of the cell suspension (~$1x10^9$ CFU/mL), each condition was assayed in duplicates completing approximately 30 individuals. The larvae were incubated at 28°C for 24 h. After this, the surviving larvae were washed and transferred to sterile E3 medium, then incubated at 28°C to complete 48 hpe. Both incubation processes were performed with the respective light/dark cycles, and in each condition, we worked with duplicates adding the control condition only with sterile E3 medium.

Bacterial colonization was recorded using an Olympus MVX10 fluorescence stereomicroscope. Prior to imaging, zebrafish larvae were anesthetized with 0.01% tricaine methanesulfonate and mounted on 1% low melting point E3-agarose plugs. For quantitative assessment of intestinal colonization, the gastrointestinal tract of the larvae was divided into three segments: anterior, middle and posterior. Based on the level of fluorescence and as was made by Marcoleta et al., 2018, four grades were established: (0) no colonization, (1) low colonization, (2) intermediate colonization and (3) high colonization. Each segment was evaluated with the mentioned colonization degrees.

Histograms were obtained by compiling the different scores obtained in the photographs using GraphPad Prism software version 8.0.1. Statistical analysis was performed with the same software using 1-way ANOVA tests using the Kruskal-Wallis test for multiple comparisons.

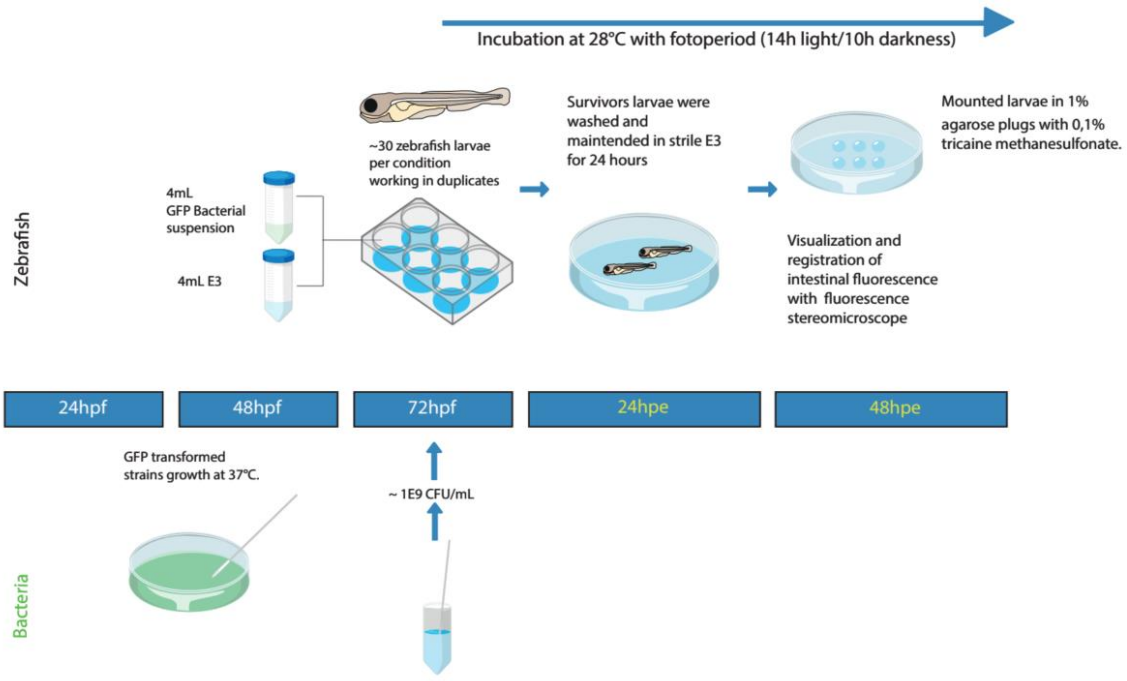

Figure 2. Workflow of the assays to evaluate the ability of SGH10, their derived mutants (ΔICEKp10, ΔGIE492, ΔICEKp10-GIE492) and pKpVP-cured strain to colonize the intestine of 72-hpf zebrafish larvae. Photographs were taken with Olympus MVX10 fluorescence stereomicroscope.

2.6 Microinjection assays

To assess neutrophil recruitment, we adapted a microinjection protocol previously described by Marcoleta et al., 2018 (Figure 3). Due to the complexity of the set-up and the technical limitations of the equipment, four strains were selected to develop this protocol. Bacterial suspensions in PBS buffer were prepared from SGH10 WT, ΔICEKp10-GIE492, KpVP-cured and Δ*wcaJ* strains transformed with the pBBRmApple plasmid, adjusting the cell concentration to reach OD600=1.4. From these suspensions, between ~$5x10^3$ and ~$1x10^4$ CFU in a volume of 3 nL were injected into the otic vesicle

of MPO:GFP transgenic larvae. A micromanipulator with needles loaded with the different suspensions was used to perform the microinjections. The procedure was made with larvae previously anesthetized with 0.01% tricaine methanesulfonate and mounted on low melting point 1% agarose plugs. At the end of the injections, each needle was discharged into a 200 µL eppendorf containing sterile PBS, with which serial dilutions were performed, and viable cells were counted on LB agar plates with Car and Kan. Control larvae were injected with sterile PBS at the same site. After the injections, the larvae were removed from their plugs to be mounted again in 1% low melting point agarose rotated 180° around their anteroposterior axis. This last step was necessary for optimal visualization of the injected vesicle in an inverted microscope setup used to perform live-cell imaging. Once the larvae were in their final position, images were captured using a Lionheart FX automated microscope (Agilent), programmed to take pictures of each larva every 10 min for 24 h in the bright field, GFP and RFP channels, in different Z-planes of the correctly infected larvae. The equipment maintained the humidity and temperature (28°C) conditions necessary for the individuals. After 24 h of monitoring, the larvae survival was recorded by visualizing the heartbeat in the heart region through the Lionheart FX microscope. Finally, the tracked individuals were dismounted from their agarose plugs to be processed and count viable cells by adapting the protocol of Mostowy et al., 2013. To do this, the larvae were removed and separated individually in 1,5 mL Eppendorf tubes, then, 100 µL of lysis buffer (Triton X-100 at 0.2% in 1X PBS buffer) were added and resuspension movements were performed with the pipette. After this, the tubes were vortexed at maximum speed for 5 min. Serial dilutions were performed in sterile PBS to count viable cells.

From the images collected using Gen5 version 3.11 software, the total fluorescence intensities of each image in the different channels were obtained, limiting the measurement only to the area circumscribed to the otic vesicle of the larvae. These data were plotted using GraphPad Prism version 8.0.1 software. Statistical analysis was performed with the same software using a mixed-effects analysis test. The lethality and bacterial load data obtained using this method of infection were plotted and subsequently analyzed statistically using 1-way ANOVA tests and subsequent multiple comparisons through the Kruskal-Wallis test.

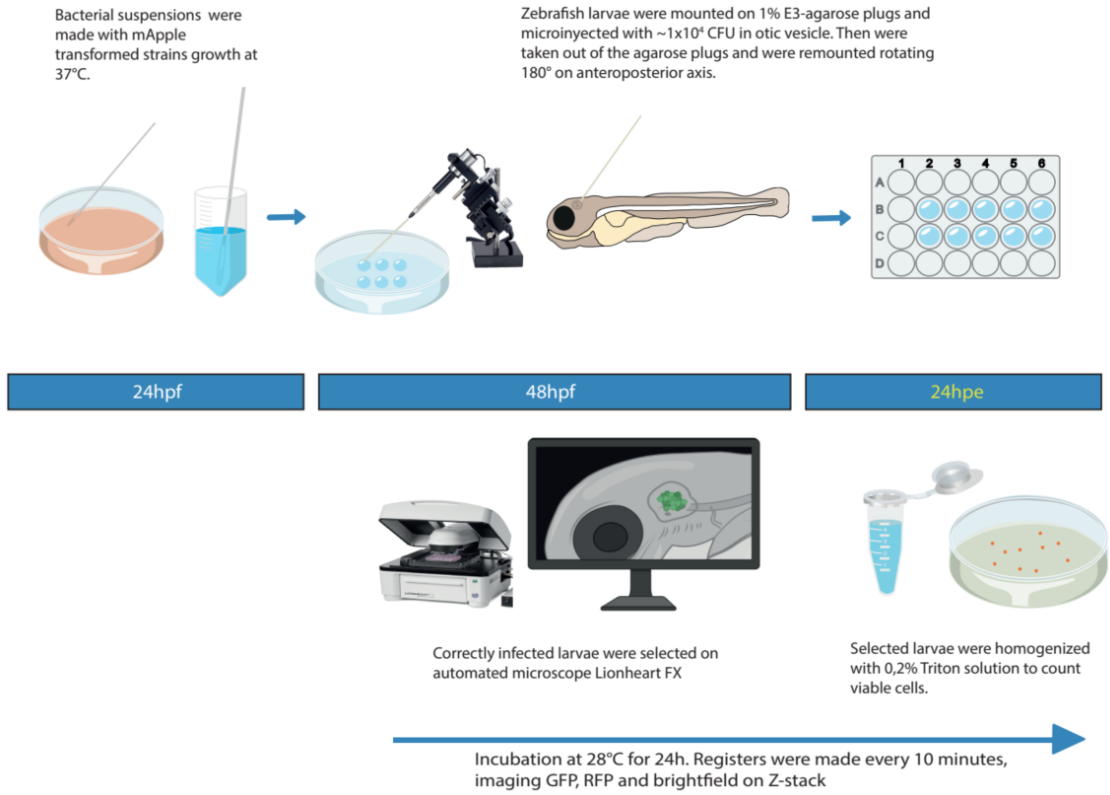

Figure 3. Workflow of the microinjection assays to evaluate the neutrophil recruitment to the otic vesicle of zebrafish larvae after infection with the SGH10 strain, the derived mutants, ΔICEKp10-GIE492, Δ*wcaJ* and pKpVP-cured strain. Monitoring was performed for 24 h using Lionheart FX automated microscope.

3. RESULTS

3.1 Role of the pKpVP, GIE492, and ICEKp10 elements in the hvKp lethality over zebrafish larvae

To determine the role of these elements, static immersion lethality experiments were performed. As negative controls, we used *K. pneumoniae* SGH10 Δ*wcaJ*, with impaired capsule production and shown to be avirulent in a murine infection model (Tan et al., 2020), and KpGe, previously shown to be avirulent over zebrafish larvae (Marcoleta et al. 2018). As expected, these control strains caused almost no lethality, while SGH10 killed roughly 70% of larvae after 24 h of infection (Figure 4). No significant differences in the killing were observed when comparing the infections made with SGH10 and the strains lacking one or more mobile genetic elements (pKpVP, ICEKp10, GIE492). Therefore, thefactors encoded in the mobile elements studied would not significantly contribute to hvKp lethality over zebrafish larvae.

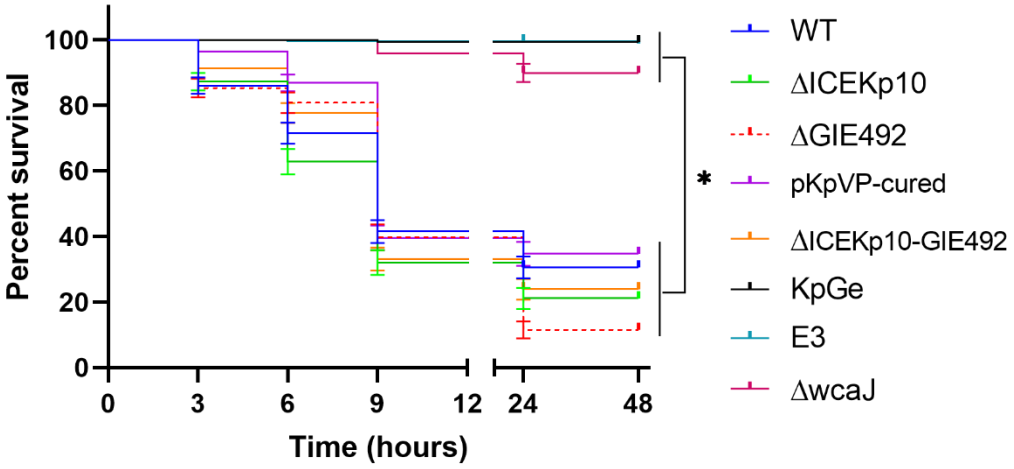

Figure 4. Zebrafish larvae survival upon hvKp infection by static immersion. Survival percentages after lethality protocols by static immersion. Statistical analysis was performed by two-way ANOVA test with multiple comparison and Bonferroni post-test. (After 10 biological replicates n= Wt 193, ΔICEKp10 156, ΔGIE492 167, pKpVP-cured 167, ΔICEKp10-GIE492 181, KpGe 165, Δ*wcaJ* 65, Control 196) (*= $p < 0.05$).

3.2 Role of pKpVP, GIE492, and ICEKp10 in the hvKp colonization of the zebrafish gut and its extra-intestinal dissemination

To compare the intestinal colonization levels of the different strains under study, a static immersion infection protocol was carried out with Tab5 larvae. In this case, 72-hpf individuals were used to minimize larval mortality and allow us to evaluate gut colonization. In order to quantify the intestinal colonization levels in the larvae, we scored the intestinal colonization according to the level of fluorescence observed in the photographs (Figure 5). Similar colonization levels were observed in the different gut segments among SGH10 and the different mutants lacking the mobile genetic elements, while only KpGe showed a significantly reduced colonization in all the tracts (Figure 6a,b,c). A similar situation was observed when comparing the total score, calculated as

the sum of the scores for the three segments of each larva (Figure 6d).

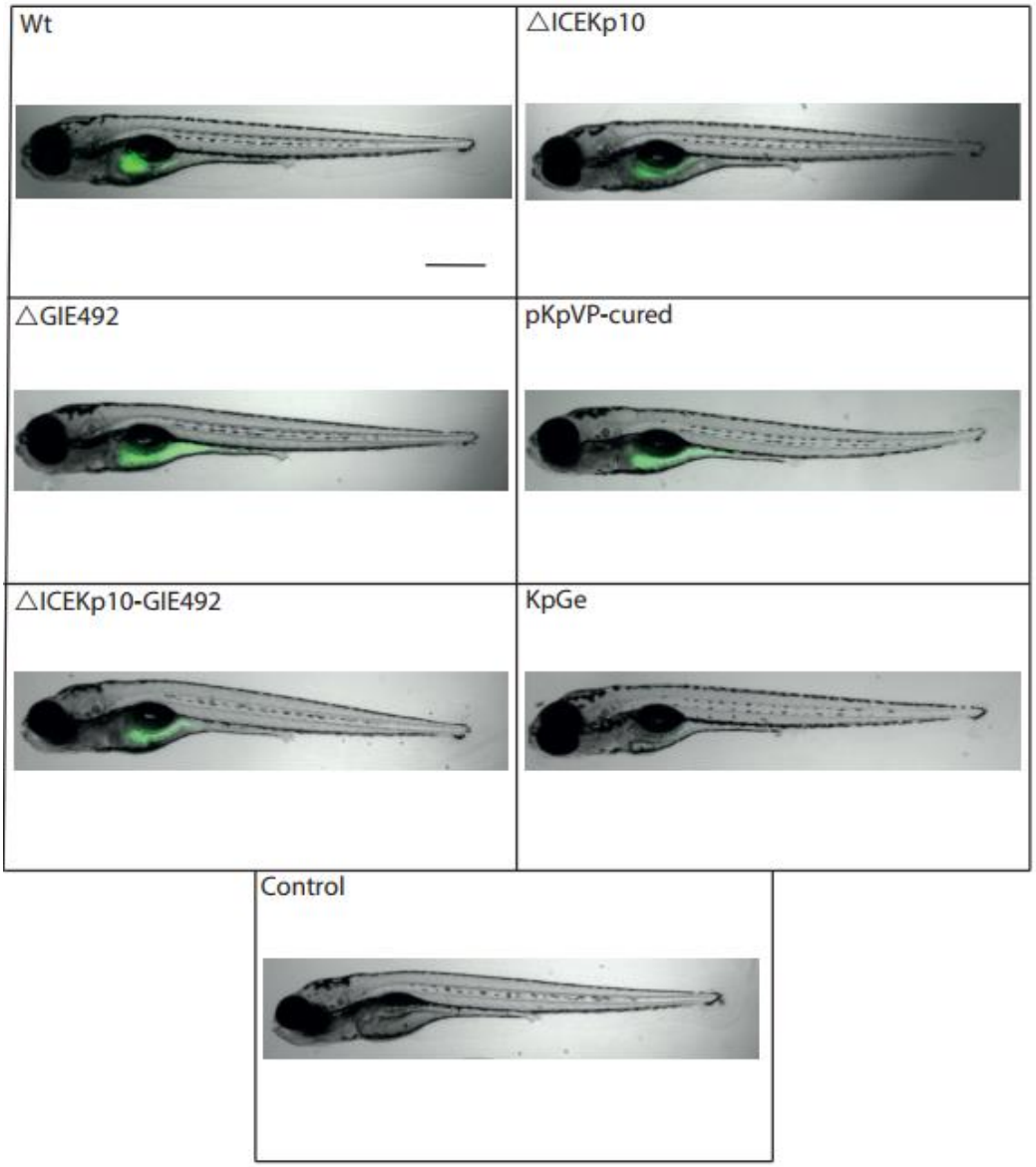

Figure 5. Representative images of intestinal colonization by *K. pneumoniae* upon zebrafish larvae infection by static immersion at 48 hpe. Scale bar: 500 µm.

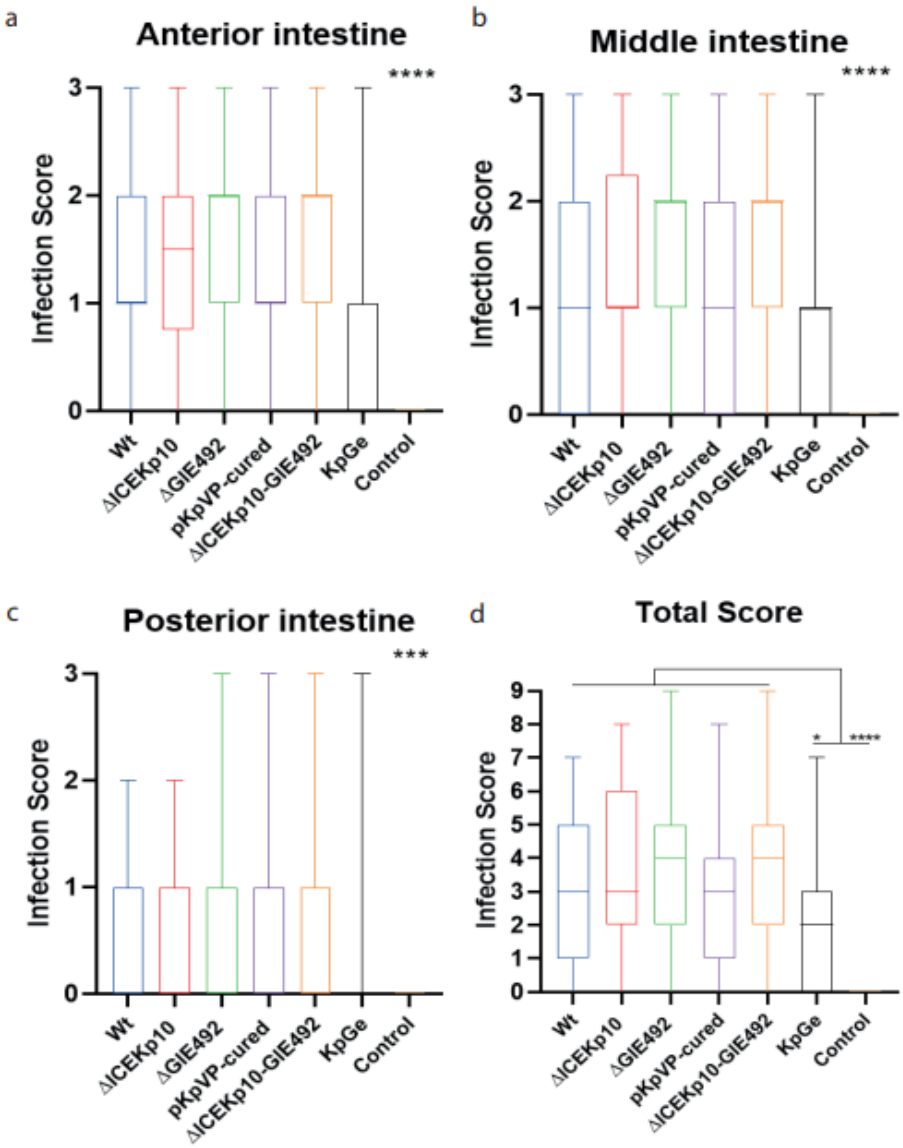

Figure 6. *K. pneumoniae* colonization of zebrafish larvae gut upon infection by static immersion. Histogram of the scores obtained for each strain in the different intestine segments. **(a)** Anterior intestine, **(b)** Middle intestine, **(c)** Posterior intestine, **(d)** Total Score. Statistical analysis was performed by 1-way ANOVA test and using the Kruskal-Wallis test for multiple comparisons. (After 7 biological replicates n= Wt 74, ΔICEKp10 74, ΔGIE492 87, pKpVP-cured 84, ΔICEKp10-GIE492 103, KpGe 98, Control 74) (*= $p < 0.05$, ***= $p = 0.0001$, ****= $p < 0.0001$).

Subsequently, the same photographic records were used to evaluate the different strains capacity to generate extra-intestinal colonization (Figure 7a). However, in this case, the occurrence of fluorescent bacteria outside the intestinal tract was evaluated (Figure 7b). Between 7 and 9% of the larvae infected either with SGH10 or the mutants lacking the mobile elements showed extra-intestinal infections, a frequency considerably higher than in the case of KpGe. This result confirms that hvKp has an increased tendency to generate this kind of infections, as observed in other animal models. The extra-intestinal infection was always accompanied by gut colonization, suggesting that the latter occurs first, followed by bacterial dissemination to other organs. Finally, the factors encoded in the genetic mobile elements studied seem to have limited relevance in the intestinal and extra-intestinal colonization of zebrafish larvae.

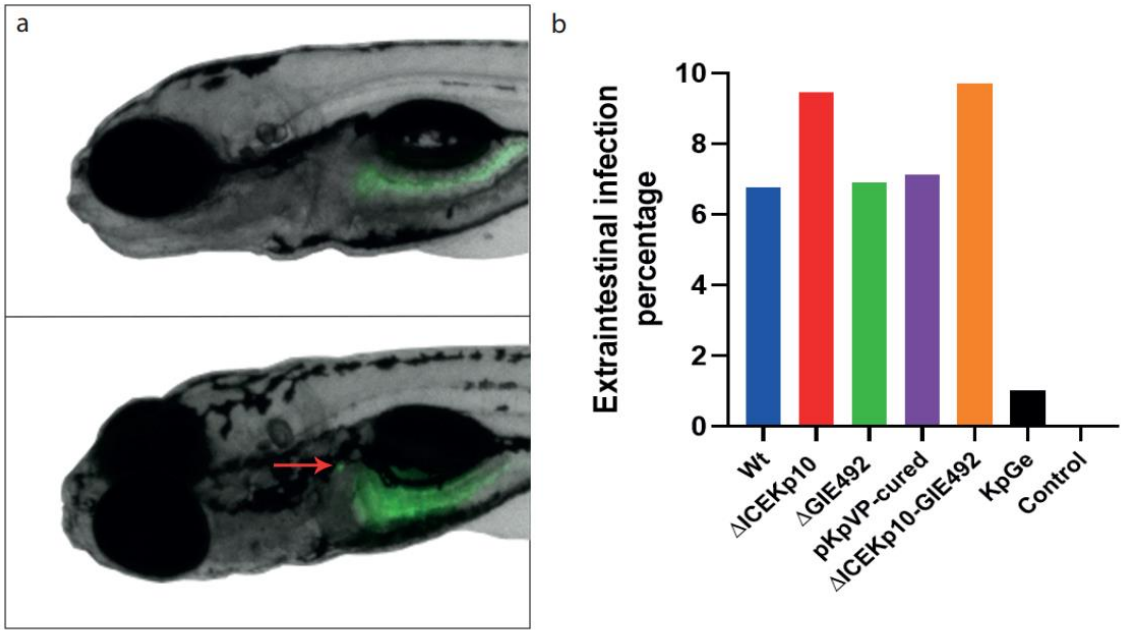

Figure 7. Zebrafish larvae extraintestinal infection by *K. pneumoniae* SGH10 and derivated strains. **(a)** Representative image of extraintestinal colonization. In the upper part, a larva with only intestinal colonization is observed. In the lower image, the point corresponding to the extraintestinal colonization developed by the individuals is marked with a red arrow. Scale bar, 500µm. **(b)** Histogram of extraintestinal infection percentages developed by zebrafish larvae during intestinal colonization assays.

3.3 Contribution of pKpVP, GIE492 and ICEKp10 to hvKp immune cell recruitment and evasion

To evaluate the zebrafish innate immune response elicited against hvKp and the mutants lacking the mobile genetic elements under study, a live-cell imaging protocol was developed, taking advantage of the optical transparency of this host model. Specifically, bacterial microinjections were performed in the otic vesicle of MPO:GFP larvae to generate localized infections with 10^4 CFU approximately. Once the larvae were injected, they were mounted on 1% LMP agarose plugs with 0.1% tricaine to be visualized through the Lionheart FX microscope, monitoring the infections for 24 h, obtaining time-lapse

images of neutrophils and the different bacterial strains. The innate immune cells recruitment upon infection and the replication capacity of SGH10, pKpVP-cured strain and the mutants ΔICEKp10-GIE492 and Δ*wcaJ* (avirulent control), were evaluated by measuring total fluorescence intensity over time. Figure 8 shows representative images of the infection time course with the different strains.

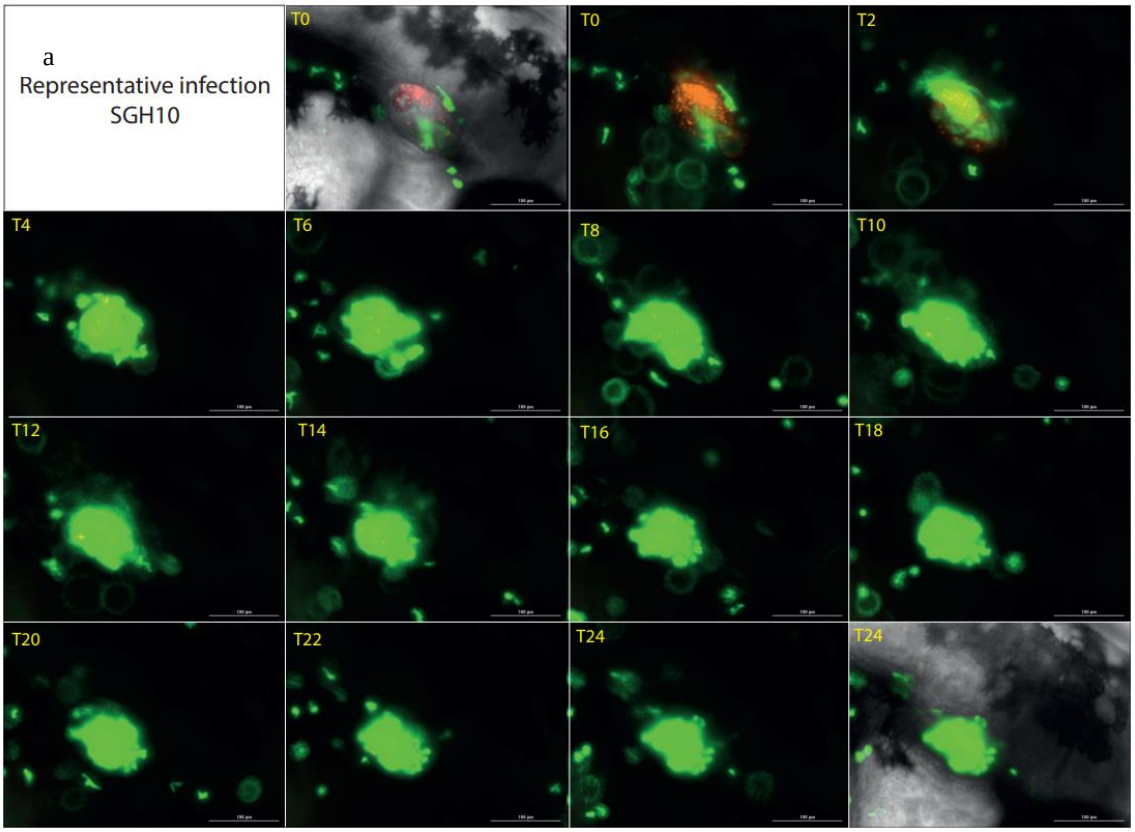

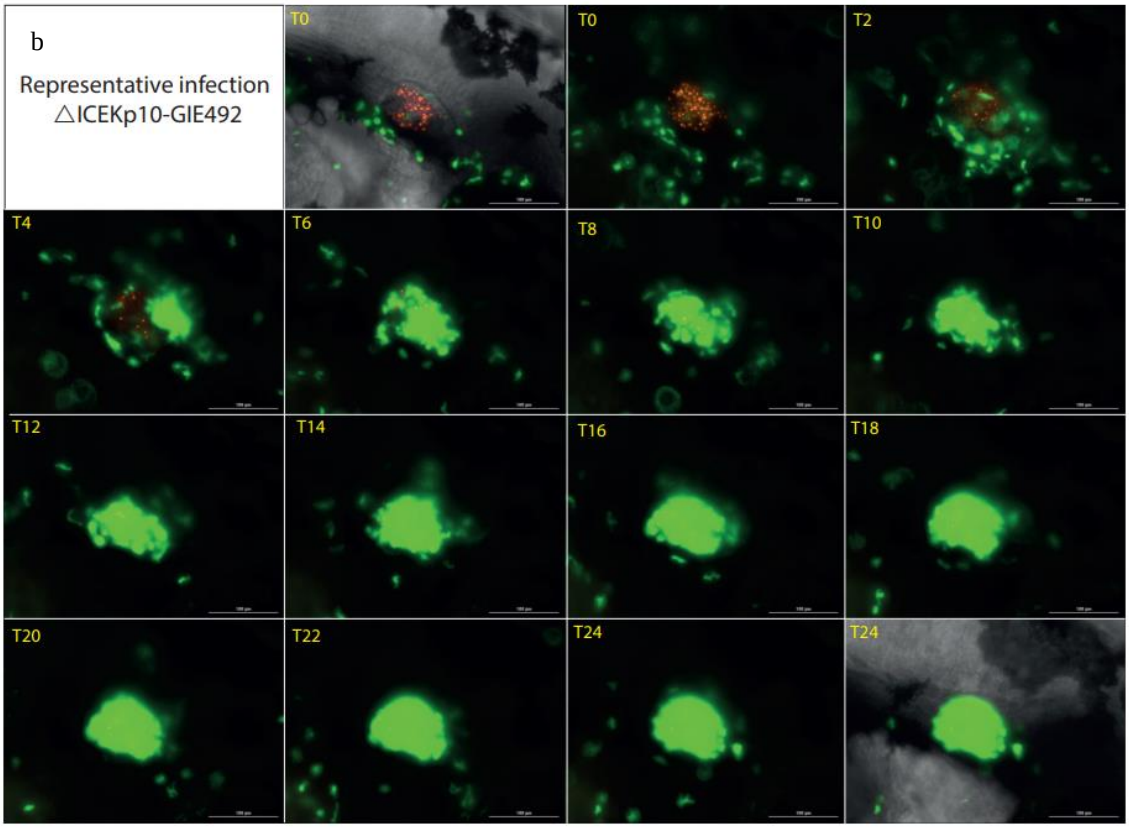
b
Representative infection
△ICEKp10-GIE492
T0
T0
T2
T4
T6
T8
T10
T12
T14
T16
T18
T20
T22
T24
T24

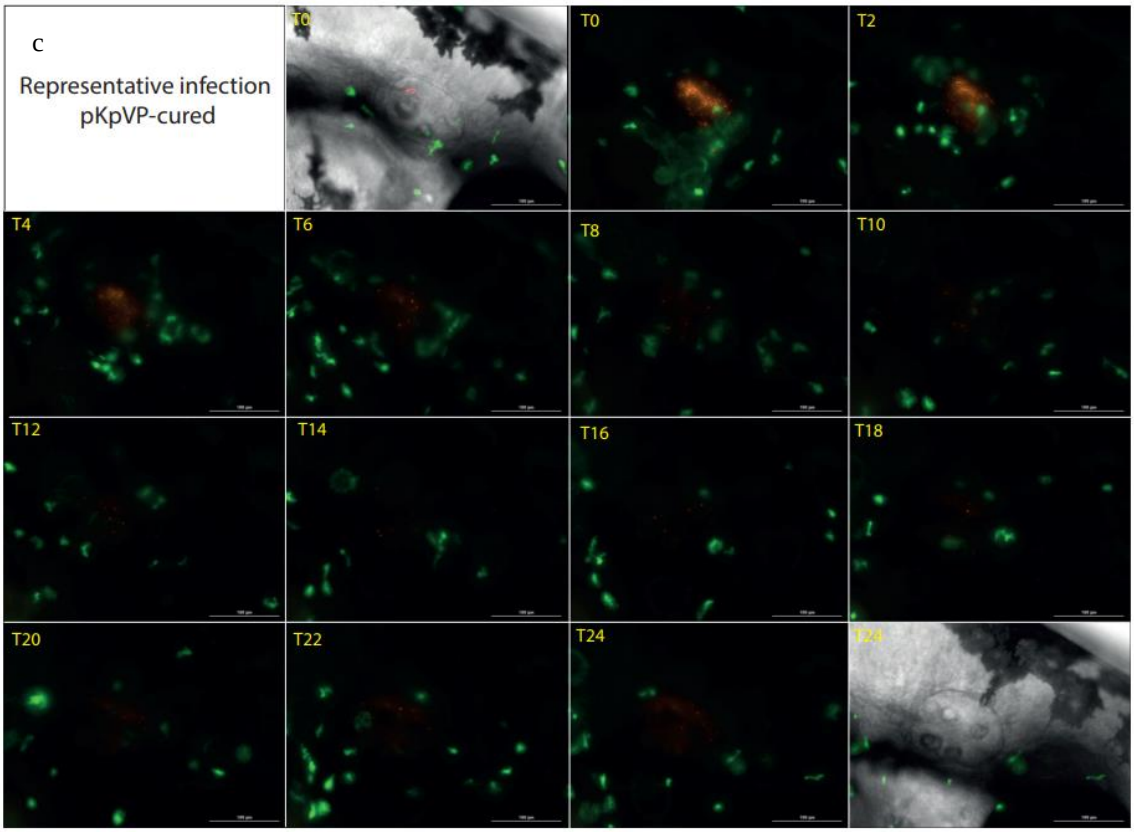
c
Representative infection
pKpVP-cured
T0
T0
T2
T4
T6
T8
T10
T12
T14
T16
T18
T20
T22
T24
T24

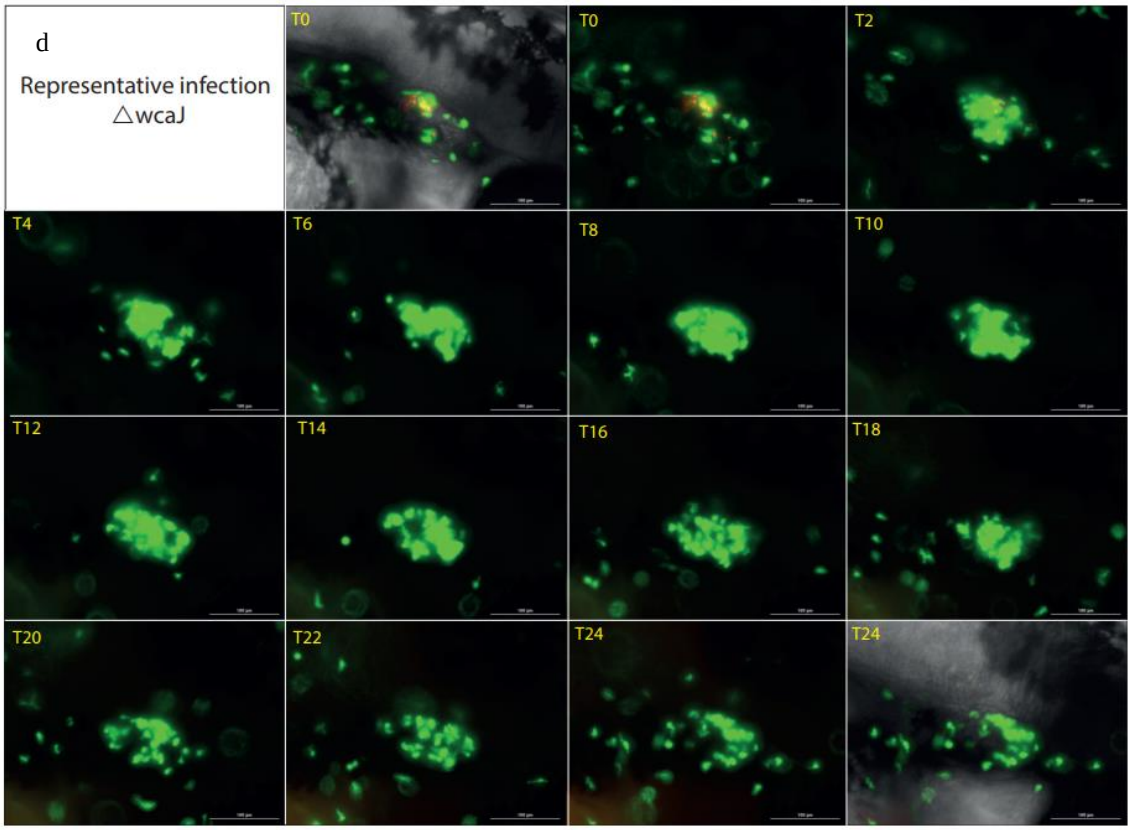
d
Representative infection
△wcaJ
T0
T0
T2
T4
T6
T8
T10
T12
T14
T16
T18
T20
T22
T24
T24

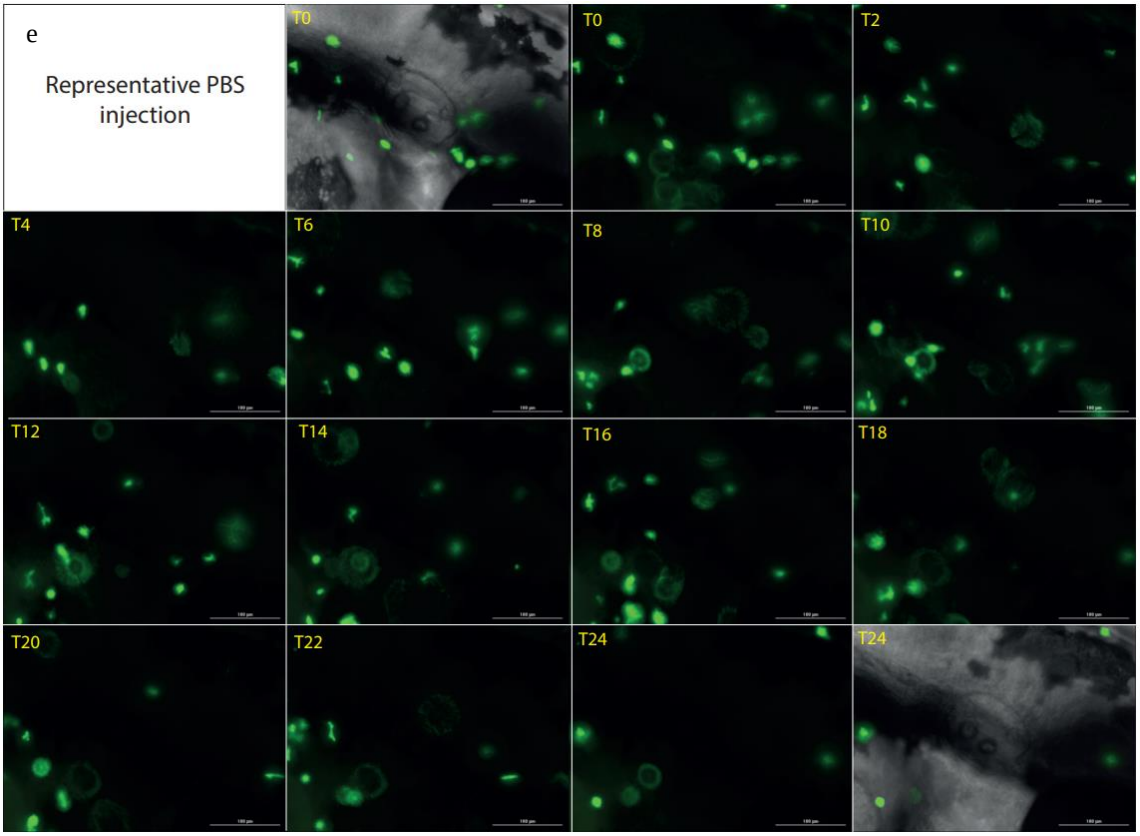

Figure 8. *In vivo* time-lapse visualization of bacterial load and neutrophil recruitment upon bacterial injection into the otic vesicle. Images show merged GFP and RFP channels every 2 h after infection (RFP: bacteria, GFP: neutrophils). Representative image series of the infection with SGH10 **(a)**, ΔICEKp10-GIE492 **(b)** pKpVP-cured **(c)**, Δ*wcaJ* **(d)**, or the mock injection with PBS **(e)** are shown.

From 8 biological replicates, 7 to 11 individuals were selected and analyzed for each condition. The total fluorescence intensity of both GFP and RFP was quantified every two hour, considering only the area circumscribed to the otic vesicle (Figure 9).

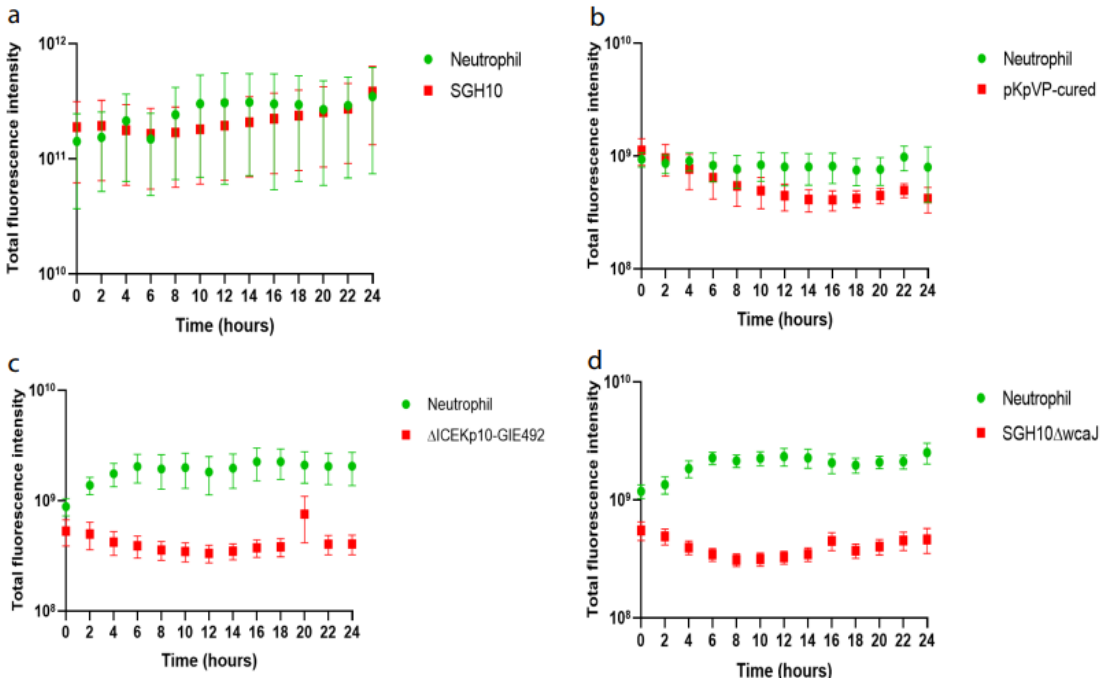

Figure 9. Total fluorescence intensity of GFP (neutrophils) and RFP (bacteria) over time upon injection of the different *K. pneumoniae* strains in the otic vesicle of zebrafish larvae.

To compare the behavior upon injection of the different bacterial strains and the subsequent neutrophil recruitment, we performed an aggregated data analysis (Figures 10 and 11). Every point in Figure 10 represents the average total green fluorescence intensity at each time, normalized by the values obtained for the mock control. The SGH10 infection showed higher neutrophil recruitment compared to the infections performed with the mutant strains, while the pKpVP-cured strain showed the lowest recruitment among the mutants. This is in agreement with the reference images, where no neutrophil confinement to the infection zone was observed at any time evaluated (Figure 8c). Figure 11 shows the total red fluorescence intensity over time of the different bacterial strains

upon injection, as a measure of bacterial load, which remained constant between the different conditions. It is also observed that the initial bacterial load of the wild-type strain would be higher than that of the rest of the strains; however, as shown in Figure 9a and Figure A2 (Annex), this phenomenon is influenced by the elevated fluorescence in GFP due to the high recruitment of neurotrophils. Therefore, the measurement of bacterial load by this approach has limitations that must be considered.

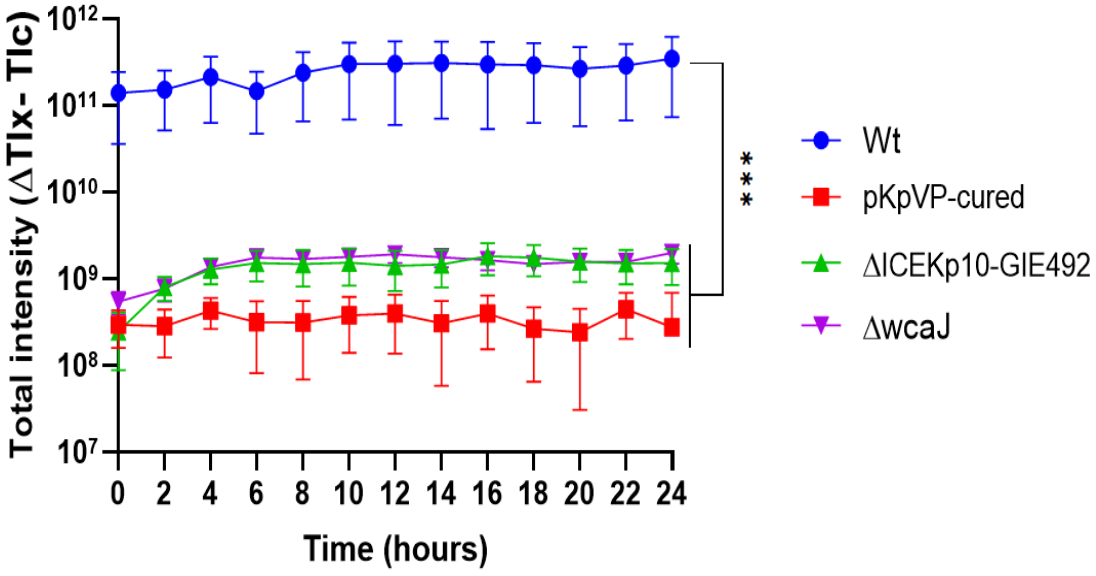

Figure 10. Total green fluorescence intensity over time of selected larvae upon bacterial injection. ΔTIx-ΔTIc represents the adjustment made to the total fluorescence intensity of the strains studied by subtracting the background fluorescence intensity obtained from the control (inoculation with PBS followed for 24 h). Statistical analysis was performed by mixed-effects analysis test. (n= Wt 10, pKpVP-cured 9, ΔICEKp10-GIE492 7, Δ*wcaJ* 9, Control 11) (***= p< 0.0001).

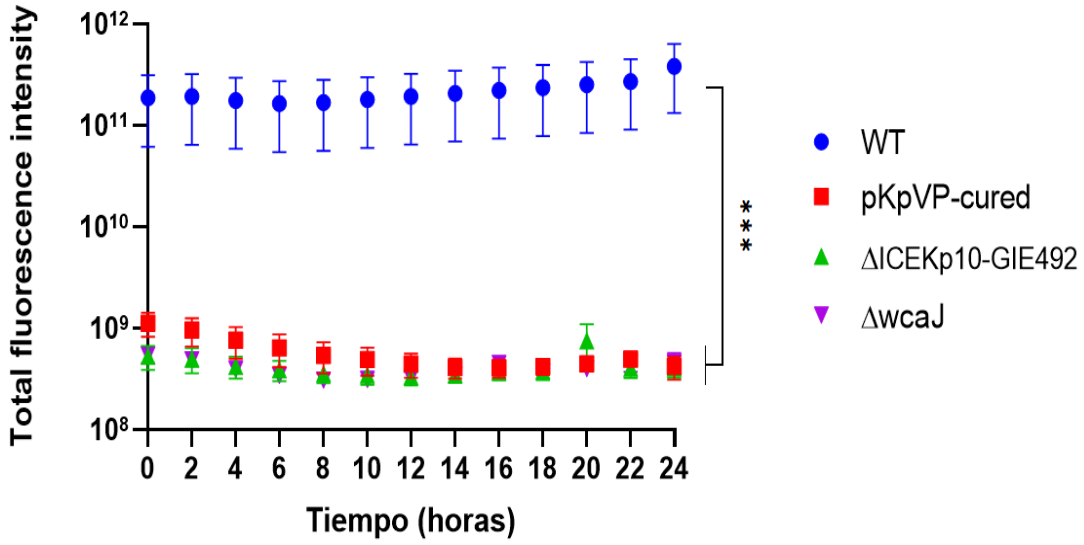

Figure 11. Total red fluorescence intensity over time of selected larvae upon bacterial injection. Statistical analysis was performed by mixed effects analysis test (n= Wt 10, pKpVP-cured 9, ΔICEKp10-GIE492 7, Δ*wcaJ* 9, Control 11) (***= p< 0.0001).

After 24 h, the survival of all the monitored individuals was recorded, and the larvae were also processed to count viable bacteria by micro drop plating on LB plates with the respective antibiotics to compare the bacterial loads. Figure 12, which shows the CFU/mL ratio after 24 h of infection by microinjection of the different strains, shows that in all cases, the bacteria can replicate and increase their number after the incubation period; however, there are no significant differences between the different treatments. In addition, the bacterial load data associated with fluorescence (Figure 11) does not agree with that observed by bacterial titers. Figure 13 shows the survival percentages of the larvae that were monitored, where it can be observed that infections with strains SGH10 and ΔICEKp10-GIE492 show similar levels of survival (50% and 41%, respectively), while

survival after infection with pKpVP-cured strain was 80%, which suggests a decrease in the virulence of this strain compared to the wild strain. Finally, infection with strain Δ*wcaJ* showed no mortality among individuals.

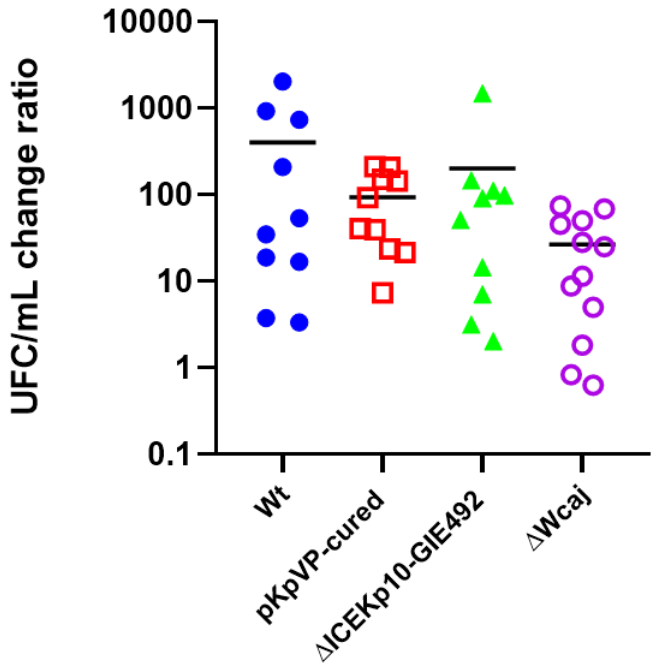

Figure 12. Ratio of change of CFU/mL in zebrafish larvae after 24 h of infection by microinjection inoculation of SGH10 strain, pKpVP-cured and ΔICEKp10-GIE492 , Δ*wcaJ* mutants. Statistical analysis was performed by 1-way ANOVA test (n= Wt 10, pKpVP-cured 10, ΔICEKp10-GIE492 11, Δ*wcaJ* 12).

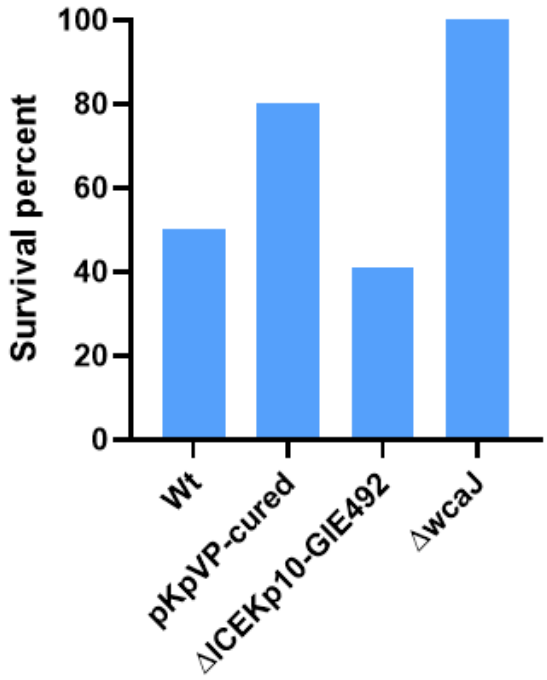

Figure 13. Percent survival of zebrafish larvae after 24 h of injection into the otic vesicle of SGH10, pKpVP-cured and mutants ΔICEKp10-GIE492 , Δ*wcaJ*. (n= Wt 10, pKpVP-cured 10, ΔICEKp10-GIE492 11, Δ*wcaJ* 12).

4. DISCUSSION

4.1 Mobile genetic elements of *Klebsiella pneumoniae* SGH10 and their relative contribution in virulence on the alternative model *Danio rerio*

Zebrafish larvae have been very useful as an alternative to the murine model to study bacterial pathogenesis because of its optical transparency and the conserved features of its innate immune system with mammals' one (Shan et al., 2015). Thus, it has been successfully used to study the virulence of *Clostridioides difficile*, *Escherichia coli*, *Salmonella enterica*, *Mycobacterium tuberculosis*, *Shigella flexneri*, and other microorganisms of global concern (Hou et al., 2016; Li et al., 2020; Mazon-Moya et al., 2017; Roca et al., 2019; Tyrkalska et al., 2016). Another microorganism of worldwide concern is *K. pneumoniae*, a species that in the last 30 years has developed multiresistant strains to antimicrobial compounds, as well as hypervirulent strains (Marr & Russo, 2019). The latter have been previously studied using the murine model and to date there is no literature describing the study of hypervirulent strains using the zebrafish model. Considering these advantages, we leveraged the zebrafish model to study the pathogenesis of hypervirulent *K. pneumoniae* SGH10 and evaluate the relative contribution of the characteristic mobile genetic elements carried by these strains in different aspects and stages of the infectious process.

In the static immersion survival assays, no significant differences were observed when comparing the wild-type strain and the mutants lacking the mobile elements, indicating

that the absence of these elements would not attenuate the killing capacity of these strains. However, significant differences were obtained when observing the survival percentages after inoculation by microinjection. In particular, the larvae infected with the pKpVP-cured strain reached 80% survival, while the wild-type and ΔICEKp10-GIE492 strains reached around 41%. The discrepancy in the results obtained between these assays may be due to an effect caused by the infection methods used. In previous work comparing the proteomic profiles of zebrafish larvae infected with *P. aeruginosa* either by static immersion or caudal artery injection, only larvae infected by static immersion presented a strong response to hypoxia through the HIF pathway (Díaz-Pascual et al., 2017). This result suggests that during the immersion in a bacterial suspension, a decrease in oxygen in the medium would occur, possibly causing additional stress and affecting the larvae health and thus the outcome of the infection.

On the other hand, no significant differences were found in the intestinal colonization levels comparing the wild-type strain and the mutants lacking the mobile elements. Additionally, there was a tendency towards less colonization in the posterior segment of the digestive tract, which may be related to the stage of development in which the individuals were used. In this regard, at 76 hpf the intestinal folds have only developed in the anterior and middle segments, and although the intestine of the larvae at this stage is already functional and has peristaltic movements, only on the seventh day post fertilization the digestive system of the larvae is fully functional (Flores et al., 2020).

Another phenomenon studied was the possible occurrence of secondary extraintestinal infections along with intestinal colonization. Although no differences were observed among the strains tested, it was possible to distinguish that all the infections observed were present in the same location. Therefore, taking into account the stage of larval development and comparing the anatomical positioning of this point with that described by Chu & Sadler, 2009, this secondary infection site would correspond to the liver of the individuals, but we do not dispose of transgenic lines or hybridization probes to corroborate this. However, another possibility is the spleen primordium, which would agree with what observed by Tu et al., 2009 in a murine model, where after intestinal colonization with a clinical isolate of *K. pneumoniae* K2 (capable of producing liver abscesses), the presence of bacteria was first observed in this organ before the liver. To date, although there is no literature describing the organogenesis of the spleen in zebrafish larvae, it is known that in adult individuals it is adjacent to one of the hepatic lobes (Menke et al., 2011), and also that the splenic veins communicate with the hepatic portal system, so it cannot be excluded that the infection observed in our images is in the spleen (Milz & Nilsson, 1969). Although it is not possible to determine which organ would be affected by this metastatic infection, these results confirm the capacity of this model as host of the hypervirulent strain SGH10 and of this pathogen to generate extraintestinal infections after colonization of the gastrointestinal tract, as observed in human infections.

Considering that the capsule and hypermucoviscosity are involved in the evasion of the host immune system (Siu et al., 2012; Walker et al., 2020), we examined the possible differences that may exist in the response of the innate immune system to infection with

the wild type strain and the mutants. For this purpose, microinjection of the different bacterial suspensions into the otic vesicle of MPO:GFP individuals was used as a method of infection in order to generate a localized infection that would allow us to observe how the cells reach the site (Sullivan et al., 2017). The infections with the mutant strains presented less neutrophil recruitment to the inoculated site than the wild type, being the pKpVP-cured strain which showed the least recruitment.

These results indicate that one or more factors encoded in the mobile genetic elements would contribute to elicit an immune host response. In this context if we look at the genomic islands, the ΔICEKp10-GIE492 mutant lacks the genomic island GIE492, which has genes to produce the salmochelin siderophores and microcin E492, and the ICEKp10 island, which has genes to produce the siderophore yersiniabactin and the genotoxin colibactin. Until now, although it is known that microcin E492 is an antimicrobial peptide that would inhibit the growth of other microorganisms competing for the same siderophores (Lagos et al., 2009), no clear role has been established during host infection. Regarding colibactin, it has been described in works associated with the murine model that, in infections associated with the digestive tract, it has had inflammatory effects due to its capacity to activate the senescence-associated secretory phenotype (SASP) (Kaur et al., 2018). Once the cells are in this state, the secretion of inflammatory cytokines (TNF-α, IL-6, IL-8, IL-1β, among others) and chemokines (GM-CSF, CCL2, 3, 4, and 5, among others) increases in nearby tissues, which are signals to initiate an immune response that includes the recruitment, infiltration and action of neutrophils (Prata et al., 2018).

On the other hand, concerning the siderophores encoded in this islands, it was previously described by Holden et al., 2015 that, in a murine infected with a *K. pneumoniae* strain associated with pneumonia, which produced both enterobactin and the two siderophores already mentioned, the presence of these three chelators induces the production of the cytokines IL-6, CXCL1 and CXCL2, where the latter two function as chemoattractants for neutrophils (Bachman, 2016; De Filippo et al., 2013). Thus, the absence of these genomic islands could reduce neutrophils recruitment to the inoculated area due to both the absence of pro-inflamatory colibactin and iron chelators that promote the production of chemoattractants for immune cells. Further studies are needed to determine the separate contribution of these islands in the neutrpohil recruitment. However, it should be noted that the pKpVP-cured strain lacking the virulence plasmid, although maintains the islands, did not produce neutrophil recruitment upon infection. This behavior can be explained by differences in the phenotype of the strains, sincethe ΔICEKp10-GIE492 strain presented slightly increased hypermucoviscocity than the wild-type strain, while the pKpVP-cured strain had lower values (see Annex, Figure A1). Thus, these results would indicate that the hypermucoviscous character of strain SGH10 is also relevant for inducing neutrophil recruitment.

After reviewing the survival of zebrafish larvae when inoculated by microinjection, it was observed that infections with the ΔICEKp10-GIE492 mutant maintained similar levels of lethality compared to the wild-type strain (Figure 13). This would indicate that the genomic islands ICEKp10 and GIE492 together would not be essential to immune response evasion and thus, this mutant is still able to survive and even propagate inside

the otic vesicle. Conversely, when infections were performed with the pKpVP-cured strain (lacking the virulence plasmid), the survival of individuals increased compared to the wild strain. This indicate that the pKpVP virulence plasmid significantly contribute to the lethality levels of the SGH10 strain. The *rmp* genes encoded in this mobile genetic element, associated with the hypermucoviscous phenotype, could account for this behavior, considering that the increased hypermucoviscosity shown by the ΔICEKp10-GIE492 strain, while the pKpVP-cured strain significantly reduces its levels (Annex, Figure A1a). This behavior is independent of the capsule production, since no significant differences were observed in the capsular polysaccharide levels among SGH10 and the mutants in mobile elements (Annex, Figure A1b).

Another possible relevant factor encoded in the pKpVP plasmid is the siderophore aerobactin, which has been described as one of the genetic markers of hypervirulent strains of *K. pneumoniae* (Guo et al., 2017; Jung et al., 2013). This iron chelator, like yersiniabactin and salmochelin, has a structure that allows it to avoid being captured by the Lipocalin 2 protein, but has the advantage of being a molecule that can be reused by the pathogen and that is capable of transferring iron from transferrin more efficiently than the siderophore enterobactin (Braun et al., 1984; Russo et al., 2015). Along with this, it should be noted that in hypervirulent *K. pneumoniae* strains, the production of aerobactin is dominant over the siderophores salmochelin and yersiniabactin, and that its absence decreases the virulence in murine infection models (Russo et al., 2014). Thus, our results indicate that, at least in the conditions tested, the virulence plasmid pKpVP would have a more relevant contribution to the infectious process, compared to the genomic islands

ICEKp10 and GIE492. However, further studies examinating further aspactes of the *K. pneumoniae* pathogenesis are needed to confirm this assertion and evaluate separately both genomic islands.

Regarding bacterial load over time upon injection into the otic vesicle, when comparing the data obtained through the photographic recording performed by the Lionheart FX automated microscope, with those obtained by plating, we found no correlation between both datasets. The first approach showed a higher bacterial load for the wild type than the rest of the strains tested, while the titration showed no such differences. Moreover the different strains proliferated after 24 h of infection, which was not observed through the fluorescence evaluation. These differences may be the result of two phenomena. One may be the limitations of using fluorescence as a measurement method. As can be seen in the Figure A2 (Annex), the high fluorescence intensity generated by the neutrophils in the GFP field produces a cross-talk with the RFP channel, causing the measurement of the bacterial load associated with the latter channel to be influenced by the fluorescence coming from the former. The second phenomenon would be related to the region measured by the different methods used. Using fluorescence limits the measurement only to the region of interest, the otic vesicle, whereas microdrop titration was performed with the whole individuals. Although, this should have a limited influence, given that the infection is localized by microinjection in the otic vesicle of the zebrafish larvae, the presence of bacteria outside this area cannot be discarded due to the dispersion capacity of the strains used.

4.2 Fluorescence as a tool for measuring bacterial colonization and immune system response

The use of fluorescence as a detection or monitoring method has been a very useful tool for biology, which is even more relevant in an organism such as the zebrafish, which, as mentioned above, has optical transparency during the first week of development. In this study, we took advantage of this condition to perform different analyses based on the fluorescence levels. First with the use of the Olympus MVX10 fluorescence stereomicroscope and a fluorescence score and then using the Lionheart FX automated microscope to obtain time-lapse images and generating quantitative measurements. In this process, where the Gen5 software was used, it was necessary to determine a measurement threshold that would allow defining an upper and lower sensitivity limit that the points analyzed had to meet to be recorded. Considering the analysis of both experiments, a common limitation was the fluorescence saturation. In this line, after a certain level of bacterial colonization or neutrophil agglomeration due to high recruitment, in some captures, the fluorescence intensity registered reached a saturated value, despite the initial parameter optimization for the capture. This implies that in a minor fraction of the captures, the total fluorescence could be underestimated , which is a limitation of the method used. However, in the case of intestinal colonization this behavior did not hinder the comparison between the different segments of the intestine, and in turn, in the case of recruitment to the otic vesicle, the events of high fluorescence intensity occur within the last stages of the infection assays performed, not interferring with the measurements in the recruitment kinetics. Therefore, although fluorescence has limitations, it still offers convenient methods to evaluate and compare bacterial virulence, especially when using

transparent host organisms. However, concerning the evaluation of bacterial load, as mentioned above and as seen in Figure 9a, the use of fluorescence-based approaches should be taken with caution, especially when a cross-talk between different fluorescence channels occur.

4.3 Infection methods comparison

In the present work, *Danio rerio* was used as the infection model, different methods were employed in this research to carry out the infections with the different strains of interest. First, we used static immersion, which consists of exposing individuals to a medium containing a bacterial suspension of a given concentration, depending on the infective dose to be achieved. This method has the advantage of being non-invasive, since the way the microorganisms enter the individual is mainly through the mouth, and then localize and colonize the digestive tract of the fish. However, it should be considered that a high concentration of bacteria in the suspension can have unfavorable effects. According to Díaz-Pascual et al. (2017), static immersion triggers a hypoxia response mediated by HIF1α in zebrafish individuals. Thus, the decrease of oxygen availability in the medium and the activation of this signaling pathway would generate a series of physiological responses, such as the induction of factors associated with inflammation, which in turn can favor iron retention by the organism. Therefore, although this method of infection is favorable for not inducing lesions in zebrafish larvae given its passive nature, it is necessary to manage the concentrations of microorganisms in the medium to avoid generating physiological responses that may affect the analysis of the data.

Another method used to perform the infections with the different strains of interest was the microinjection of bacterial suspensions into the otic vesicle of the larvae to generate a localized inoculation. Compared to static immersion, the advantages of this method lie in the fact that no response to hypoxia would be generated because the bacteria are not in the medium and the number of bacteria used is much smaller, which means that there is no induction of the HIF pathway. Therefore, the results observed are not influenced by the physiological responses generated by this process. However, it may be noted that although inoculation can be carried out with a small number of bacteria, it is difficult to control the number of CFU injected. Also it should not be forgotten that this process implies physical damage to the larvae due to the use of capillaries that must break the epithelial tissue to discharge the microorganisms. Previous reports indicate that tissue damage can cause neutrophil-mediated inflammation in the area (Mathias et al., 2006; Myllymäki et al., 2022). However, this effect can be compensated with the use of control infections where a harmless substance is injected, and thus the potential neutrophil recruitment can be considered when evaluating the effects caused by the strains or conditions of interest.

As it has been described, the different infection methods used in this research have advantages and disadvantages, which must be considered to correctly evaluate the conditions of interest.

CONCLUSIONS

1) Zebrafish is a suitable model to study hypervirulent *K. penumoniae* pathogenesis.

2) The mobile elements pKpVP, ICEKp10, and GIE492 are not essential for lethality and zebrafish gut colonization upon immersion in a bacterial suspension.

3) Hypervirulent *K. pneumoniae* SGH10 have increased capacity to establish extraintestinal infections upon zebrafish gut colonization, recapitulating what is observed in mammalian host models.

4) One or more factors encoded in the pKpVP virulence plasmid contributes to the lethality of hvKp SGH10 over zebrafish larvae.

5) As a method of infection to study hypervirulent *K. pneumoniae* pathogenesis using zebrafish, microinjection has advantages over static immersion because the inoculation of individuals can be controlled without developing secondary responses associated with hypoxia.

Bibliography

Astin, J. W., Keerthisinghe, P., Du, L., Sanderson, L. E., Crosier, K. E., Crosier, P. S., & Hall, C. J. (2017). Innate immune cells and bacterial infection in zebrafish. *Methods in Cell Biology*, *138*, 31–60. https://doi.org/10.1016/bs.mcb.2016.08.002

Bachman, M. A. (2016). Dissemination , and HIF-1 ␣ Stabilization during Pneumonia. *mBio 7(5):E01397-16.* https://doi.org/10.1128/mBio.01397-16.

Benard, E. L., van der Sar, A. M., Ellett, F., Lieschke, G. J., Spaink, H. P., & Meijer, A. H. (2012). Infection of zebrafish embryos with intracellular bacterial pathogens. *Journal of Visualized Experiments : JoVE*, *61*, 1–8. https://doi.org/10.3791/3781

Braun, V., Brazel-Faisst, C., & Schneider, R. (1984). Growth stimulation of *Escherichia coli* in serum by iron(III) aerobactin. Recycling of aerobactin. *FEMS Microbiology Letters*, *21*(1), 99–103. https://doi.org/10.1111/j.1574-6968.1984.tb00193.x

Casadevall, A., & Pirofski, L. A. (2009). Virulence factors and their mechanisms of action: The view from a damage-response framework. *Journal of Water and Health*, *7*(SUPPL. 1), 2–18. https://doi.org/10.2166/wh.2009.036

Chaves, J., Ladona, M. G., Segura, C., Coira, A., Reig, R., & Ampurdanés, C. (2001). SHV-1 β-lactamase is mainly a chromosomally encoded species-specific enzyme in *Klebsiella pneumoniae*. *Antimicrobial Agents and Chemotherapy*, *45*(10), 2856–2861. https://doi.org/10.1128/AAC.45.10.2856-2861.2001

Choby, J. E., Howard-Anderson, J., & Weiss, D. S. (2020). Hypervirulent *Klebsiella pneumoniae* – clinical and molecular perspectives. *Journal of Internal Medicine*, *287*(3), 283–300. https://doi.org/10.1111/joim.13007

Chu, J., & Sadler, K. C. (2009). New school in liver development: Lessons from zebrafish. *Hepatology*, *50*(5), 1656–1663. https://doi.org/10.1002/hep.23157

De Filippo, K., Dudeck, A., Hasenberg, M., Nye, E., Van Rooijen, N., Hartmann, K., Gunzer, M., Roers, A., & Hogg, N. (2013). Mast cell and macrophage chemokines CXCL1/CXCL2 control the early stage of neutrophil recruitment during tissue inflammation. *Blood*, *121*(24), 4930–4937. https://doi.org/10.1182/blood-2013-02-486217

Decré, D., Verdet, C., Emirian, A., Le Gourrierec, T., Petit, J. C., Offenstadt, G., Maury, E., Brisse, S., & Arlet, G. (2011). Emerging severe and fatal infections due to *Klebsiella pneumoniae* in two university hospitals in France. *Journal of Clinical*

Microbiology, *49*(8), 3012–3014. https://doi.org/10.1128/JCM.00676-11

Díaz-Pascual, F., Ortíz-Severín, J., Varas, M. A., Allende, M. L., & Chávez, F. P. (2017). In vivo host-pathogen interaction as revealed by global proteomic profiling of zebrafish larvae. *Frontiers in Cellular and Infection Microbiology*, *7*(JUL), 1–11. https://doi.org/10.3389/fcimb.2017.00334

Faïs, T., Delmas, J., Barnich, N., Bonnet, R., & Dalmasso, G. (2018). Colibactin: More than a new bacterial toxin. *Toxins*, *10*(4), 16–18. https://doi.org/10.3390/toxins10040151

Fierer, J., Walls, L., & Chu, P. (2011). Recurring *Klebsiella pneumoniae* pyogenic liver abscesses in a resident of San Diego, California, due to a K1 strain carrying the virulence plasmid. *Journal of Clinical Microbiology*, *49*(12), 4371–4373. https://doi.org/10.1128/JCM.05658-11

Flores, E. M., Nguyen, A. T., Odem, M. A., Eisenhoffer, G. T., & Krachler, A. M. (2020). The zebrafish as a model for gastrointestinal tract–microbe interactions. *Cellular Microbiology*, *22*(3). https://doi.org/10.1111/cmi.13152

Guo, Y., Wang, S., Zhan, L., Jin, Y., Duan, J., Hao, Z., Lv, J., Qi, X., Chen, L., Kreiswirth, B. N., Wang, L., & Yu, F. (2017). Microbiological and clinical characteristics of hypermucoviscous *Klebsiella pneumoniae* isolates associated with invasive infections in China. *Frontiers in Cellular and Infection Microbiology*, *7*(FEB), 1–9. https://doi.org/10.3389/fcimb.2017.00024

Harvie, E. A., & Huttenlocher, A. (2015). Neutrophils in host defense: new insights from zebrafish. *Journal of Leukocyte Biology*, *98*(4), 523–537. https://doi.org/10.1189/jlb.4mr1114-524r

Herbomel, P. (1999). Spinning nuclei in the brain of the zebrafish embryo [1]. *Current Biology*, *9*(17), 3735–3745. https://doi.org/10.1016/S0960-9822(99)80407-2

Hider, R. C., & Kong, X. (2010). *Chemistry and biology of siderophores †‡*. 637–657. https://doi.org/10.1039/b906679a

Holden, V. I., Bachman, M. A., & Holden, V. I. (2015). Diverging roles of bacterial siderophores during infection biology and Immunology with. *Metallomics*, *7*, 986–995. https://doi.org/10.1039/C4MT00333K

Hou, Y., Sheng, Z., Mao, X., Li, C., Chen, J., Zhang, J., Huang, H., Ruan, H., Luo, L., & Li, L. (2016). Systemic inoculation of *Escherichia coli* causes emergency myelopoiesis in zebrafish larval caudal hematopoietic tissue. *Scientific Reports*, *6*(February), 1–14. https://doi.org/10.1038/srep36853

Howe, K., Clark, M. D., Torroja, C. F., Torrance, J., Berthelot, C., Muffato, M., Collins, J. E., Humphray, S., McLaren, K., Matthews, L., McLaren, S., Sealy, I., Caccamo, M., Churcher, C., Scott, C., Barrett, J. C., Koch, R., Rauch, G. J., White, S., Chow,

W., Kilian, B., Quintais, L. T., Guerra-Assunção, J. A., Zhou, Y., Gu, Y., Yen, J., Vogel, J. H., Eyre, T., Redmond, S., Banerjee, R., Chi, J., Fu, B., Langley, E., Maguire, S. F., Laird, G. K., Lloyd, D., Kenyon, E., Donaldson, S., Sehra, H., Almeida-King, J., Loveland, J., Trevanion, S., Jones, M., Quail, M., Willey, D., Hunt, A., Burton, J., Sims, S., McLay, K., Plumb, B., Davis, J., Clee, C., Oliver, K., Clark, R., Riddle, C., Eliott, D., Threadgold, G., Harden, G., Ware, D., Mortimer, B., Kerry, G., Heath, P., Phillimore, B., Tracey, A.,Corby, N., Dunn, M., Johnson, C., Wood, J., Clark, S., Pelan, S., Griffiths, G., Smith, M., Glithero, R., Howden, P., Barker, N., Stevens, C., Harley, J., Holt, K., Panagiotidis, G., Lovell, J., Beasley, H., Henderson, C., Gordon, D., Auger, K., Wright, D., Collins, J., Raisen, C., Dyer, L., Leung, K., Robertson, L., Ambridge, K., Leongamornlert, D., McGuire, S., Gilderthorp, R., Griffiths, C., Manthravadi, D., Nichol, S., Barker, G., Whitehead, S., Kay, M., Brown, J., Murnane, C., Gray, E., Humphries, M., Sycamore, N., Barker, D., Saunders, D., Wallis, J., Babbage, A., Hammond, S., Mashreghi-Mohammadi, M., Barr, L., Martin, S., Wray, P., Ellington, A., Matthews, N., Ellwood, M., Woodmansey, R., Clark, G., Cooper, J., Tromans, A., Grafham, D., Skuce, C., Pandian, R., Andrews, R., Harrison, E., Kimberley, A., Garnett, J., Fosker, N., Hall, R., Garner, P., Kelly, D., Bird, C., Palmer, S., Gehring, I., Berger, A., Dooley, C. M., Ersan-Ürün, Z., Eser, C., Geiger, H., Geisler, M., Karotki, L., Kirn, A., Konantz, J., Konantz, M., Oberländer, M., Rudolph-Geiger, S., Teucke, M., Osoegawa, K., Zhu, B., Rapp, A., Widaa, S., Langford, C., Yang, F., Carter, N. P., Harrow, J., Ning, Z., Herrero, J., Searle, S.M.J., Enright, A., Geisler, R., Plasterk, R.H.A., Lee, C., Westerfield, M., De Jong, P.J., Zon, L.I., Postlethwait, J.H., Nüsslein-Volhard, C., Hubbard, T.J.P., Crollius, H.R., Rogers, J., Stemple, D.L. Stemple, D. L. (2013). The zebrafish reference genome sequence and its relationship to the human genome. *Nature*, *496*(7446), 498–503. https://doi.org/10.1038/nature12111

Johnson, D. I. (2017). Bacterial pathogens and their virulence factors. In *Bacterial Pathogens and Their Virulence Factors*. https://doi.org/10.1007/978-3-319-67651-7

Jung, S. W., Chae, H. J., Park, Y. J., Yu, J. K., Kim, S. Y., Lee, H. K., Lee, J. H., Kahng, J. M., Lee, S. O., Lee, M. K., Lim, J. H., Lee, C. H., Chang, S. J., Ahn, J. Y., Lee, J. W., & Park, Y. G. (2013). Microbiological and clinical characteristics of bacteraemia caused by the hypermucoviscosity phenotype of *Klebsiella pneumoniae* in Korea. *Epidemiology and Infection*, *141*(2), 334–340. https://doi.org/10.1017/S0950268812000933

Kaur, C. P., Vadivelu, J., & Chandramathi, S. (2018). Impact of *Klebsiella pneumoniae* in lower gastrointestinal tract diseases. *Journal of Digestive Diseases*, *19*(5), 262–271. https://doi.org/10.1111/1751-2980.12595

Lagos, R., Tello, M., Mercado, G., Garcia, V., & Monasterio, O. (2009). Antibacterial and Antitumorigenic Properties of Microcin E492, a Pore- Forming Bacteriocin. *Current Pharmaceutical Biotechnology*, *10*(1), 74–85. https://doi.org/10.2174/138920109787048643

Lagos, Rosalba, Wilkens, M., Vergara, C., Cecchi, X., & Monasterio, O. (1993). Microcin E492 forms ion channels in phospholipid bilayer membranes. *FEBS Letters*, *321*(2–3), 145–148. https://doi.org/10.1016/0014-5793(93)80096-D

Lam, M. M. C., Wyres, K. L., Duchêne, S., Wick, R. R., Judd, L. M., Gan, Y. H., Hoh, C. H., Archuleta, S., Molton, J. S., Kalimuddin, S., Koh, T. H., Passet, V., Brisse, S., & Holt, K. E. (2018). Population genomics of hypervirulent *Klebsiella pneumoniae* clonal-group 23 reveals early emergence and rapid global dissemination. *Nature Communications*, *9*(1). https://doi.org/10.1038/s41467-018-05114-7

Lam, M. M. C., Wyres, K. L., Judd, L. M., Wick, R. R., Jenney, A., Brisse, S., & Holt, K. E. (2018). Tracking key virulence loci encoding aerobactin and salmochelin siderophore synthesis in *Klebsiella pneumoniae*. *Genome Medicine*, *10*(1), 1–15. https://doi.org/10.1186/s13073-018-0587-5

Li, J., Ünal, C. M., Namikawa, K., Steinert, M., & Köster, R. W. (2020). Development of a larval zebrafish infection model for Clostridioides difficile. *Journal of Visualized Experiments*, *2020*(156), 1–7. https://doi.org/10.3791/60793

Malachowa, N., & Deleo, F. R. (2010). Mobile genetic elements of *Staphylococcus aureus*. *Cellular and Molecular Life Sciences*, *67*(18), 3057–3071. https://doi.org/10.1007/s00018-010-0389-4

Marcoleta, A. E., Varas, M. A., Ortiz-Severín, J., Vásquez, L., Berríos-Pastén, C., Sabag, A. V., Chávez, F. P., Allende, M. L., Santiviago, C. A., Monasterio, O., & Lagos, R. (2018). Evaluating different virulence traits of *Klebsiella pneumoniae* using *Dictyostelium discoideum* and zebrafish larvae as host models. *Frontiers in Cellular and Infection Microbiology*, *8*(FEB), 1–20. https://doi.org/10.3389/fcimb.2018.00030

Marr, C. M., & Russo, T. A. (2019). Hypervirulent *Klebsiella pneumoniae*: a new public health threat. *Expert Review of Anti-Infective Therapy*, *17*(2), 71–73. https://doi.org/10.1080/14787210.2019.1555470

Mathias, J. R., Perrin, B. J., Liu, T.-X., Kanki, J., Look, A. T., & Huttenlocher, A. (2006). Resolution of inflammation by retrograde chemotaxis of neutrophils in transgenic zebrafish. *Journal of Leukocyte Biology*, *80*(6), 1281–1288. https://doi.org/10.1189/jlb.0506346

Mazon-Moya, M. J., Willis, A. R., Torraca, V., Boucontet, L., Shenoy, A. R., Colucci-Guyon, E., & Mostowy, S. (2017). Septins restrict inflammation and protect zebrafish larvae from *Shigella* infection. *PLoS Pathogens*, *13*(6), 1–22. https://doi.org/10.1371/journal.ppat.1006467

Meeker, N. D., & Trede, N. S. (2008). Immunology and zebrafish: Spawning new models of human disease. *Developmental and Comparative Immunology*, *32*(7), 745–757. https://doi.org/10.1016/j.dci.2007.11.011

Menke, A. L., Spitsbergen, J. M., Wolterbeek, A. P. M., & Woutersen, R. A. (2011). Normal anatomy and histology of the adult zebrafish. *Toxicologic Pathology*, *39*(5), 759–775. https://doi.org/10.1177/0192623311409597

Milz, D., & Nilsson, S. (1969). *(Fänge & Nilsson 1985) The fish spleen - Structure and function*. 152–158.

Mostowy, S., Boucontet, L., Mazon Moya, M. J., Sirianni, A., Boudinot, P., Hollinshead, M., Cossart, P., Herbomel, P., Levraud, J. P., & Colucci-Guyon, E. (2013). The Zebrafish as a New Model for the In Vivo Study of *Shigella flexneri* Interaction with Phagocytes and Bacterial Autophagy. *PLoS Pathogens*, *9*(9). https://doi.org/10.1371/journal.ppat.1003588

Myllymäki, H., Yu, P. (Pearl), & Feng, Y. (2022). Opportunities presented by zebrafish larval models to study neutrophil function in tissues. *International Journal of Biochemistry and Cell Biology*, *148*(June). https://doi.org/10.1016/j.biocel.2022.106234

Paczosa, M. K., & Mecsas, J. (2016). *Klebsiella pneumoniae*: Going on the Offense with a Strong Defense. *Microbiology and Molecular Biology Reviews*, *80*(3). https://doi.org/10.1128/mmbr.00078-15

Pan, Y. J., Lin, T. L., Chen, C. T., Chen, Y. Y., Hsieh, P. F., Hsu, C. R., Wu, M. C., & Wang, J. T. (2015). Genetic analysis of capsular polysaccharide synthesis gene clusters in 79 capsular types of *Klebsiella* spp. *Scientific Reports*, *5*(October 2014), 1–10. https://doi.org/10.1038/srep15573

Pendleton, J. N., Gorman, S. P., & Gilmore, B. F. (2013). Clinical relevance of the ESKAPE pathogens. *Expert Review of Anti-Infective Therapy*, *11*(3), 297–308. https://doi.org/10.1586/eri.13.12

Podschun, R., & Ullmann, U. (1998). *Klebsiella* spp. as nosocomial pathogens: Epidemiology, taxonomy, typing methods, and pathogenicity factors. *Clinical Microbiology Reviews*, *11*(4), 589–603. https://doi.org/10.1128/cmr.11.4.589

Prata, L. G. P. L., Ovsyannikova, I. G., Tchkonia, T., & Kirkland, J. L. (2018). Senescent cell clearance by the immune system: Emerging therapeutic opportunities. *Seminars in Immunology*, *40*(April). https://doi.org/10.1016/j.smim.2019.04.003

Prokesch, B. C., TeKippe, M., Kim, J., Raj, P., TeKippe, E. M. E., & Greenberg, D. E. (2016). Primary osteomyelitis caused by hypervirulent *Klebsiella pneumoniae*. *The Lancet Infectious Diseases*, *16*(9), e190–e195. https://doi.org/10.1016/S1473-3099(16)30021-4

Renshaw, S. A., Loynes, C. A., Trushell, D. M. I., Elworthy, S., Ingham, P. W., & Whyte, M. K. B. (2006). Atransgenic zebrafish model of neutrophilic inflammation. *Blood*, *108*(13), 3976–3978. https://doi.org/10.1182/blood-2006-05-024075

Riley, M. A., & Gordon, D. M. (1999). The ecological role of bacteriocins in bacterial competition. *Trends in Microbiology*, *7*(3), 129–133. https://doi.org/10.1016/S0966-842X(99)01459-6

Roca, F. J., Whitworth, L. J., Redmond, S., Jones, A. A., & Ramakrishnan, L. (2019). TNF Induces Pathogenic Programmed Macrophage Necrosis in Tuberculosis through a Mitochondrial-Lysosomal-Endoplasmic Reticulum Circuit. *Cell*, *178*(6), 1344-1361.e11. https://doi.org/10.1016/j.cell.2019.08.004

Russo, T. A., Olson, R., MacDonald, U., Beanan, J., & Davidsona, B. A. (2015). Aerobactin, but not yersiniabactin, salmochelin, or enterobactin, enables the growth/survival of hypervirulent (hypermucoviscous) *Klebsiella pneumoniae* ex vivo and in vivo. *Infection and Immunity*, *83*(8), 3325–3333. https://doi.org/10.1128/IAI.00430-15

Russo, T. A., Olson, R., Macdonald, U., Metzger, D., Maltese, L. M., & Drake, E. J. (n.d.). *Aerobactin Mediates Virulence and Accounts for Increased Siderophore Production under Iron-Limiting Conditions by Hypervirulent (Hypermucoviscous) Klebsiella pneumoniae*. *22*. https://doi.org/10.1128/IAI.01667-13

Saha, R., Saha, N., Donofrio, R. S., & Bestervelt, L. L. (2012). *Review Microbial siderophores : a mini review*. 1–15. https://doi.org/10.1002/jobm.201100552

Saraceni, P. R., Romero, A., Figueras, A., & Novoa, B. (2016). Establishment of infection models in zebrafish larvae (Danio rerio) to study the pathogenesis of *Aeromonas hydrophila*. *Frontiers in Microbiology*, *7*(AUG), 1–14. https://doi.org/10.3389/fmicb.2016.01219

Shan, Y., Fang, C., Cheng, C., Wang, Y., Peng, J., & Fang, W. (2015). Immersion infection of germ-free zebrafish with *Listeria monocytogenes* induces transient expression of innate immune response genes. *Frontiers in Microbiology*, *6*(APR), 1–11. https://doi.org/10.3389/fmicb.2015.00373

Shon, A. S., Bajwa, R. P. S., & Russo, T. A. (2013). Hypervirulent (hypermucoviscous) *Klebsiella Pneumoniae*: A new and dangerous breed. *Virulence*, *4*(2), 107–118. https://doi.org/10.4161/viru.22718

Siu, L. K., Yeh, K. M., Lin, J. C., Fung, C. P., & Chang, F. Y. (2012). *Klebsiella pneumoniae* liver abscess: A new invasive syndrome. *The Lancet Infectious Diseases*, *12*(11), 881–887. https://doi.org/10.1016/S1473-3099(12)70205-0

Stein, C., Caccamo, M., Laird, G., & Leptin, M. (2007). Conservation and divergence of gene families encoding components of innate immune response systems in zebrafish. *Genome Biology*, *8*(11). https://doi.org/10.1186/gb-2007-8-11-r251

Sullivan, C., Matty, M. A., Jurczyszak, D., Gabor, K. A., Millard, P. J., Tobin, D. M., & Kim, C. H. (2017). Infectious disease models in zebrafish. In *Methods in Cell Biology*

(Vol. 138). Elsevier Ltd. https://doi.org/10.1016/bs.mcb.2016.10.005

Taieb, F., Petit, C., Nougayrède, J.-P., & Oswald, E. (2016). The Enterobacterial Genotoxins: Cytolethal Distending Toxin and Colibactin. *EcoSal Plus*, *7*(1). https://doi.org/10.1128/ecosalplus.esp-0008-2016

Tan, Y. H., Chen, Y., Chu, W. H. W., Sham, L. T., & Gan, Y. H. (2020). Cell envelope defects of different capsule-null mutants in K1 hypervirulent *Klebsiella pneumoniae* can affect bacterial pathogenesis. *Molecular Microbiology*, *January*, 1–17. https://doi.org/10.1111/mmi.14447

Torraca, V., Masud, S., Spaink, H. P., & Meijer, A. H. (2014). Macrophage-pathogen interactions in infectious diseases: New therapeutic insights from the zebrafish host model. *DMM Disease Models and Mechanisms*, *7*(7), 785–797. https://doi.org/10.1242/dmm.015594

Tu, Y. C., Lu, M. C., Chiang, M. K., Huang, S. P., Peng, H. L., Chang, H. Y., Jan, M. S., & Lai, Y. C. (2009). Genetic requirements for *Klebsiella pneumoniae*-induced liver abscess in an oral infection model. *Infection and Immunity*, *77*(7), 2657–2671. https://doi.org/10.1128/IAI.01523-08

Turton, J. F., Englender, H., Gabriel, S. N., Turton, S. E., Kaufmann, M. E., & Pitt, T. L. (2007). Genetically similar isolates of *Klebsiella pneumoniae* serotype K1 causing liver abscesses in three continents. *Journal of Medical Microbiology*, *56*(5), 593–597. https://doi.org/10.1099/jmm.0.46964-0

Tyrkalska, S. D., Candel, S., Angosto, D., Gómez-Abellán, V., Martín-Sánchez, F., García-Moreno, D., Zapata-Pérez, R., Sánchez-Ferrer, Á., Sepulcre, M. P., Pelegrín, P., & Mulero, V. (2016). Neutrophils mediate *Salmonella Typhimurium* clearance through the GBP4 inflammasome-dependent production of prostaglandins. *Nature Communications*, *7*. https://doi.org/10.1038/ncomms12077

Varas, M., Fariña, A., Díaz-Pascual, F., Ortíz-Severín, J., Marcoleta, A. E., Allende, M. L., Santiviago, C. A., & Chávez, F. P. (2017). Live-cell imaging of *Salmonella Typhimurium* interaction with zebrafish larvae after injection and immersion delivery methods. *Journal of Microbiological Methods*, *135*, 20–25. https://doi.org/10.1016/j.mimet.2017.01.020

Vergunst, A. C., & O'Callaghan, D. (2014). Host-Bacteria Interactions. *Methods in Molecular Biology 1197*, *1197*. https://doi.org/10.1007/978-1-4939-1261-2

Vila, A. (2011). Appearance of *Klebsiella Pneumoniae* Liver Abscess Syndrome in Argentina: Case Report and Review of Molecular Mechanisms of Pathogenesis. *The Open Microbiology Journal*, *5*(1), 107–113. https://doi.org/10.2174/1874285801105010107

Walker, K. A., Treat, L. P., & Miller, V. L. (2020). The small protein RmpD drives

hypermucoviscosity in *Klebsiella pneumoniae*. *BioRxiv*, *11*(5), 1–14. https://doi.org/10.1101/2020.01.08.899096

Wang, Z., Lin, L., Chen, W., Zheng, X., Zhang, Y., Liu, Q., & Yang, D. (2019). Neutrophil plays critical role during *Edwardsiella piscicida* immersion infection in zebrafish larvae. *Fish and Shellfish Immunology*, *87*(February), 565–572. https://doi.org/10.1016/j.fsi.2019.02.008

Westerfield, M. (2000). *The zebrafish book: a guide for the laboratory use of zebrafish (Danio rerio)* (4th ed.). University of Oregon press.

Wyres, K. L., Lam, M. M. C., & Holt, K. E. (2020). Population genomics of *Klebsiella pneumoniae*. *Nature Reviews Microbiology*, *18*(6), 344–359. https://doi.org/10.1038/s41579-019-0315-1

Ye, M., Tu, J., Jiang, J., Bi, Y., You, W., Zhang, Y., Ren, J., Zhu, T., Cao, Z., Yu, Z., Shao, C., Shen, Z., Ding, B., Yuan, J., Zhao, X., Guo, Q., Xu, X., Huang, J., & Wang, M. (2016). Clinical and genomic analysis of liver abscess-causing *Klebsiella pneumoniae* identifies new liver abscess-associated virulence genes. *Frontiers in Cellular and Infection Microbiology*, *6*(NOV), 1–12. https://doi.org/10.3389/fcimb.2016.00165

Yeh, K. M., Lin, J. C., Yin, F. Y., Fung, C. P., Hung, H. C., Siu, L. K., & Chang, F. Y. (2010). Revisiting the importance of virulence determinant maga and its surrounding genes in *Klebsiella pneumoniae* causing pyogenic liver abscesses: Exact role in serotype k1 capsule formation. *Journal of Infectious Diseases*, *201*(8), 1259–1267. https://doi.org/10.1086/606010

Annex

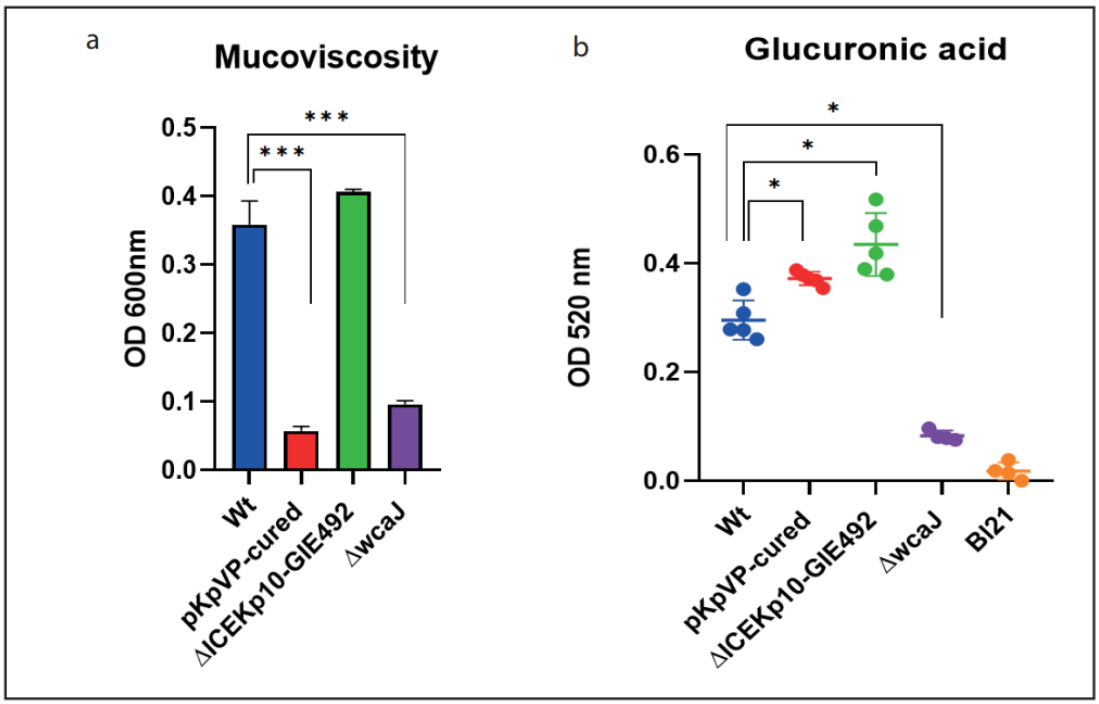

Figure A1. Evaluation of hypermucoviscocity and capsular polysaccharide production in SGH10 and derived mutants. **a.** Optical density measurements of mucoviscosity from low-speed centrifugation of bacterial strain cultures. **b.** Capsule measurements of strains from glucuronic acid extraction

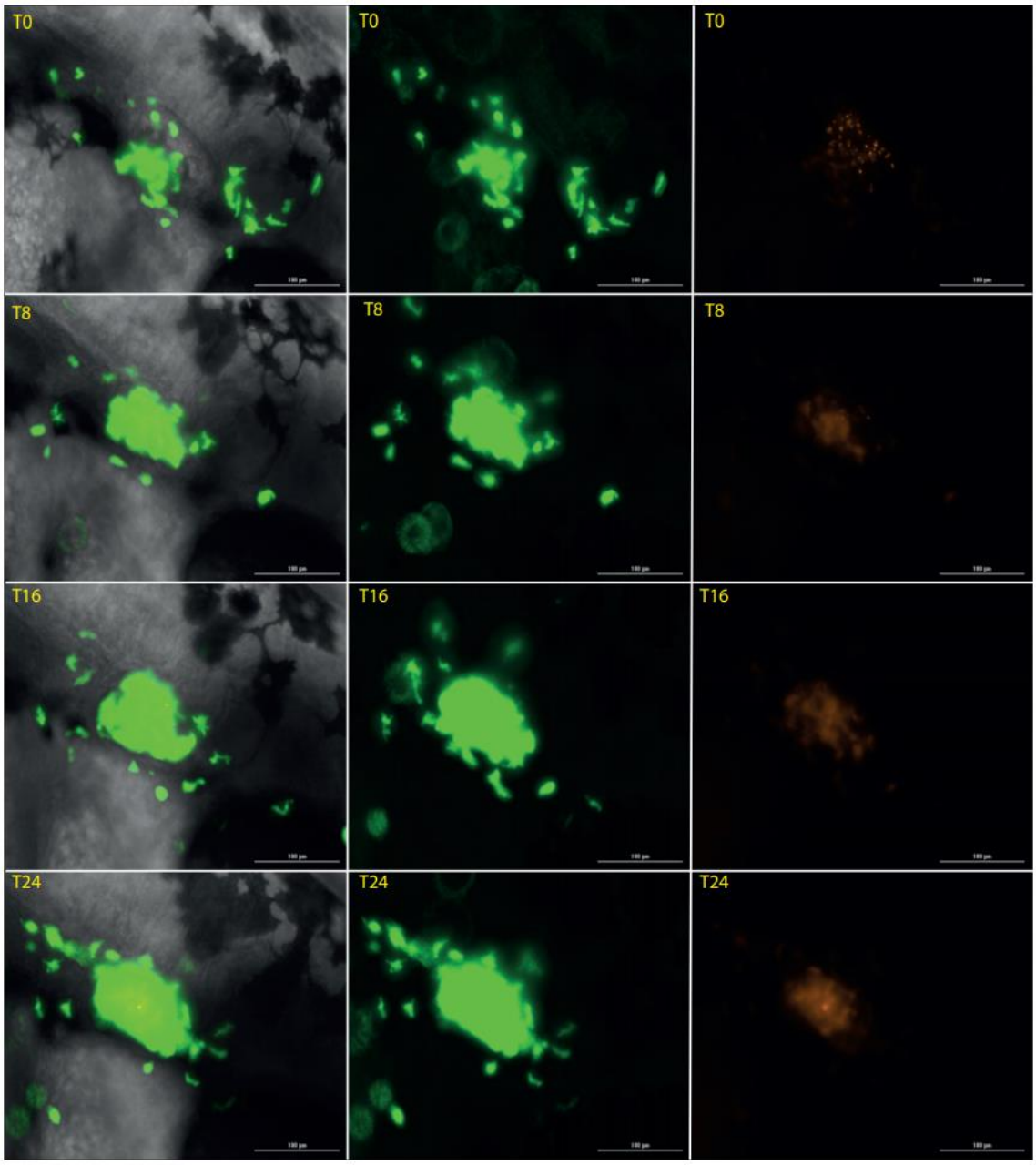

Figure A2. Representative image of infection with SGH10 strain in otic vesicle by microinjection. The bright field and the GFP (neutrophils) and RFP (bacteria) fields are observed at different times.